

*Digital Comprehensive Summaries of Uppsala Dissertations  
from the Faculty of Science and Technology 2313*

# Diving Deep into Saturn's Equatorial Ionosphere with Cassini

*Insights from the Grand Finale*

JOSHUA DREYER



ACTA UNIVERSITATIS  
UPSALIENSIS  
2023

ISSN 1651-6214  
ISBN 978-91-513-1910-0  
urn:nbn:se:uu:diva-512834



UPPSALA  
UNIVERSITET

Dissertation presented at Uppsala University to be publicly examined in Sonja Lyttkens (101121), Ångströmlaboratoriet, Lagerhyddsvägen 1, Uppsala, Thursday, 23 November 2023 at 13:00 for the degree of Doctor of Philosophy. The examination will be conducted in English. Faculty examiner: Professor Ingo Müller-Wodarg (Imperial College London, UK).

### Abstract

Dreyer, J. 2023. Diving Deep into Saturn's Equatorial Ionosphere with Cassini. Insights from the Grand Finale. *Digital Comprehensive Summaries of Uppsala Dissertations from the Faculty of Science and Technology* 2313. 59 pp. Uppsala: Acta Universitatis Upsaliensis. ISBN 978-91-513-1910-0.

In the summer of 2017, the *Cassini* mission concluded its nearly 13 years orbiting Saturn with a series of daring dives between the rings and the upper reaches of Saturn's atmosphere. This last phase of the mission, called the *Grand Finale*, revealed a highly variable equatorial ionosphere dominated by a large influx of ring material from Saturn's D ring. The papers included in this thesis utilize data gathered during these proximal orbits to gain insights into the nature and effects of the infalling ring material.

Initially, we derive upper limits for the effective recombination coefficient in Saturn's equatorial ionosphere at altitudes below 2500 km, where photochemical equilibrium can be assumed, to constrain the composition of the positive ion species. Our inceptive results indicate that ion species with low recombination coefficients are dominant.

We follow up on this by developing a photochemical model, incorporating grain charging, to investigate the effects of the ring influx on the plasma composition. The model results at an altitude of 1700 km yield vastly different abundances of two types of neutral species when compared to those derived from measurements, ultimately representing the difficulty of reconciling the observed  $H^+$  and  $H_3^+$  densities with our and other model results.

Exploring the nature of narrow decreases in the ionospheric  $H_2^+$  densities reveals a time shift in the ion data. After correcting for this, the decreases line up very well with calculated shadows for substructures in Saturn's C ring. We can further estimate the optical depths of these substructures and investigate at which altitudes photochemical equilibrium for  $H_2^+$  is applicable.

The direct measurement of heavier neutral species during the proximal orbits is complicated by the high spacecraft speed. We devise a method to utilize helium ion chemistry to independently derive the mixing ratios of these heavier neutrals in Saturn's ionosphere. Our results show considerable variability, which may suggest temporal and/or spatial changes in the ring influx. A comparison with other studies indicates that potentially only the most volatile ring-sourced species significantly ablate to enter the gas phase in this region of Saturn's ionosphere.

Finally, we compare the fixed-bias Langmuir probe electron densities and the light ion densities. They exhibit a strong positive correlation for most parts of the proximal orbits even on short timescales. We find three distinct regions in the proximal orbits, which can provide further insight into the ionospheric composition, connection to the rings, and measurement uncertainties.

*Keywords:* Saturn, Cassini, Grand Finale, Ionosphere, Photochemistry, Planetary Rings, Planetary Science, Space Plasma, Space Physics

*Joshua Dreyer, Department of Physics and Astronomy, Box 516, Uppsala University, SE-751 20 Uppsala, Sweden. Swedish Institute of Space Physics, Uppsala Division, Box 537, Uppsala University, SE-75121 Uppsala, Sweden.*

© Joshua Dreyer 2023

ISSN 1651-6214

ISBN 978-91-513-1910-0

URN urn:nbn:se:uu:diva-512834 (<http://urn.kb.se/resolve?urn=urn:nbn:se:uu:diva-512834>)

*To the wondrous wanderers  
and the wandering wonderers*

*And to those who teach*



# List of papers

This thesis is based on the following papers, which are referred to in the text by their Roman numerals.

- I *Constraining the Positive Ion Composition in Saturn's Lower Ionosphere with the Effective Recombination Coefficient*  
**Dreyer, J.**, Vigren, E., Morooka, M., Wahlund, J.-E., Buchert S. C., Johansson, F. L., and Waite, J. H. (2021)  
The Planetary Science Journal 2.1, p. 39. DOI: 10.3847/psj/abd6e9
- II *Empirical Photochemical Modeling of Saturn's Ionization Balance Including Grain Charging*  
Vigren, E., **Dreyer, J.**, Eriksson, A. I., Johansson, F. L., Morooka, M., and Wahlund, J.-E. (2022)  
The Planetary Science Journal 3.2, p. 49. DOI: 10.3847/psj/ac4eee
- III *Identifying Shadowing Signatures of C Ring Ringlets and Plateaus in Cassini Data from Saturn's Ionosphere*  
**Dreyer, J.**, Vigren, E., Johansson, F. L., Shebanits, O., Morooka, M., Wahlund, J.-E., Perryman, R. S., and Waite, J. H. (2022)  
The Planetary Science Journal 3.7, p. 168. DOI: 10.3847/psj/ac7790
- IV *Utilizing Helium Ion Chemistry to Derive Mixing Ratios of Heavier Neutral Species in Saturn's Equatorial Ionosphere*  
**Dreyer, J.**, Vigren, E., Johansson, F. L., and Waite, J. H. (2023)  
Journal of Geophysical Research: Space Physics 128.6, e2023JA031488. DOI: 10.1029/2023ja031488
- V *Electron to Light Ion Density Ratios During Cassini's Grand Finale: Addressing Open Questions About Saturn's Low-latitude Ionosphere*  
**Dreyer, J.**, Vigren, E., Johansson, F. L., Hadid, L., Morooka, M., Wahlund, J.-E., and Waite, J. H.  
Manuscript in preparation

Reprints were made with permission from the publishers.

# List of papers not included in this thesis

**Dreyer, J.**, Partamies, N., Whiter, D., Ellingsen, P. G., Baddeley, L., and Buchert, S. C. (2021)

*Characteristics of fragmented aurora-like emissions (FAEs) observed on Svalbard*, *Annales Geophysicae*, 39.2, 277–288. DOI: 10.5194/angeo-39-277-2021

Whiter, D. K., Sundberg, H., Lanchester, B. S., **Dreyer, J.**, Partamies, N., Ivchenko, N., Zaccaria Di Fraia, M., Oliver, R., Serpell-Stevens, A., Shaw-Diaz, T., and Braunersreuther, T. (2021)

*Fine-scale dynamics of fragmented aurora-like emissions*, *Annales Geophysicae*, 39.6, 975–989. DOI: 10.5194/angeo-39-975-2021

Johansson, F. L., Vigren, E., Waite, J. H., Miller, K., Eriksson, A. I., Edberg, N. J. T., and **Dreyer, J.** (2022)

*Implications from secondary emission from neutral impact on Cassini plasma and dust measurements*, *Monthly Notices of the Royal Astronomical Society*, 515.2, 2340–2350. DOI: 10.1093/mnras/stac1856

This PhD thesis is partially based on the licentiate dissertation "*Saturn's dusty equatorial ionosphere from Cassini's Grand Finale observations*" by J. Dreyer, Uppsala University, 2021. All chapters have been edited and updated to varying extents. Chapters 1, 3, 4, 5, and 7 were revised and extended, and Chapter 6 was updated to include the more recent papers. Chapters 2 and 8 are new.

# Contents

1	Introduction .....	9
2	Some Basics of Planetary Ionospheres .....	12
2.1	Photochemistry .....	13
2.2	Example of a simple photochemical model .....	13
3	Saturn and its Rings .....	16
3.1	Pre-Cassini models and observations .....	16
3.2	Ring rain to mid-latitudes .....	19
3.3	Revelations from Cassini prior to the Grand Finale .....	19
3.4	Saturn's rings .....	20
4	Insights from Cassini's Grand Finale .....	24
4.1	Proximal orbits .....	24
4.2	Ring influx around the equatorial plane .....	25
4.3	New models of Saturn's ionosphere .....	29
5	Instrumentation .....	32
5.1	Radio and Plasma Wave Science (RPWS) .....	32
5.1.1	Langmuir probe (LP) .....	33
5.2	Ion and Neutral Mass Spectrometer (INMS) .....	36
6	Summary of Publications .....	39
6.1	Paper I .....	39
6.2	Paper II .....	40
6.3	Paper III .....	41
6.4	Paper IV .....	42
6.5	Paper V .....	43
7	Outlook .....	44
8	Sammanfattning på svenska .....	46
	Acknowledgements .....	49
	References .....	51

# Acronyms and units

$\alpha_{300}$	effective recombination coefficient at 300 K
$\text{\AA}$	Ångström $\equiv 0.1$ nm
<b>ASI</b>	Agenzia Spaziale Italiana (Italian Space Agency)
<b>Da</b>	Dalton $\equiv$ unified atomic mass unit (u)
<b>ESA</b>	European Space Agency
<b>EUV</b>	Extreme Ultraviolet
<b>eV</b>	electronvolt $\approx 1.602 \times 10^{-19}$ joules
<b>INMS</b>	Ion and Neutral Mass Spectrometer
<b>IRF</b>	Institutet för Rymdfysik (Swedish Institute of Space Physics)
<b>ISS</b>	Imaging Science System
<b>JPL</b>	Jet Propulsion Laboratory
<b>LP</b>	Langmuir Probe
<b>NASA</b>	National Aeronautics and Space Administration
<b>PCE</b>	Photochemical Equilibrium
<b>ppm</b>	parts per million
<b>RPWS</b>	Radio and Plasma Wave Science
<b>SEE</b>	Solar EUV Experiment
<b>TIMED</b>	Thermosphere, Ionosphere, Mesosphere Energetics and Dynamics
<b>UVIS</b>	Ultraviolet Imaging Spectrograph

# 1. Introduction

When talking about the beauty of space and specifically our own neighbourhood, Saturn and its ring system are often named together as perhaps the most stunning feature of our solar system. But they are more than just a visually inspiring bundle deal. Saturn has long been known to shape its rings – and they are shaping parts of Saturn as well. Their connection goes beyond a purely spatial contiguity based on gravitational interactions, as the rings are connected to Saturn’s atmosphere via an inward stream of particles and thus play a major role in the physical and chemical processes within.

The second-largest planet in our solar system is large enough to have been known to humanity for our entire recorded history. Its current English name is a sign of the giant’s prominence in the classical antiquity, referring to the Roman god Saturnus, which itself is the approximate equivalent of the Greek titan Kronos, lending the still commonly used term *Kronian*. Despite the planet being observed for millennia, the rings of Saturn are not discernible without the use of a reasonably powerful telescope, and thus were not reported as such prior to their observation by the Dutch scientist Christiaan Huygens, who published his findings in 1659. Rather amusingly, Galileo Galilei had observed the rings in 1610, but due to the limitations of his telescopes, he simply noted that the planet seemed to have *ears*. In 1675, the Italian-French astronomer Giovanni Domenico Cassini was the first to observe gaps within the rings.

Our understanding of the Kronian system has evolved much in the past 400 years, initially steadily alongside the advances in telescope technology, and then rapidly with the onset of the space age. Early observations from the flybys

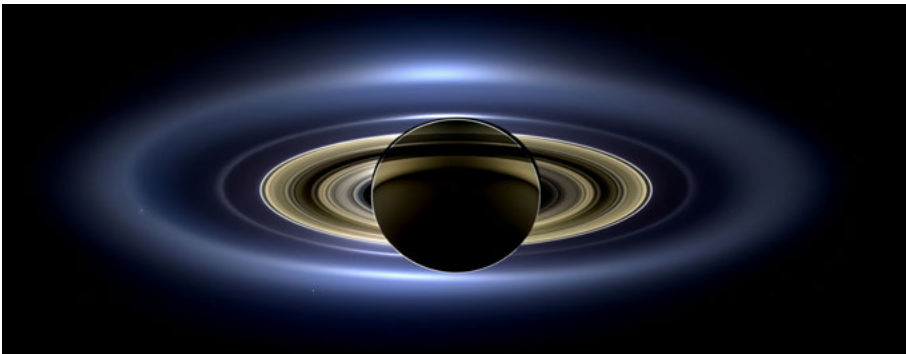


*Figure 1.1.* A mosaic of Cassini images depicting Saturn and its rings. Image credit: NASA/JPL-Caltech

of the Pioneer 11 and two Voyager probes in 1979–1981 showed the ringed giant unprecedented clarity, revealing new moons, rings and a much closer connection between these constituents of the system than previously thought. Saturn then enjoyed a prolonged period of quiescence before humanity once again decided to pay it a visit. The joined NASA/ESA/ASI *Cassini-Huygens* mission, named after the aforementioned astronomers, was a Flagship mission to Saturn and its largest moon, Titan. It was to study the giant and its local environment more extensively and closely than previous flybys had allowed. After its launch aboard a Titan IV-B rocket on 15 October 1997 and nearly seven years of travel through the solar system, the Cassini-Huygens spacecraft arrived in orbit around Saturn in July 2004. This marked the beginning of a 13-year period of new insights and discoveries. During this time, it extensively studied Saturn, its rings, satellites, and their environment, utilizing a wide array of onboard instruments. This included a series of Titan flybys and the delivery of the Huygens probe, which descended into the moon’s thick and hazy atmosphere in January 2005, after which the mission continued under the name *Cassini*. Its journey around Saturn was divided into a series of missions. The *Prime Mission* initially lasted from July 2004 to June 2008. This was followed by the two-year *Equinox* and the seven-year *Solstice Missions*, the latter of which was to culminate with the depletion of the propellant. Various proposals for potential science objectives for the end of its lifetime were assessed. Ultimately, it was decided that a series of daring dives between Saturn’s atmosphere and its rings would maximize the scientific gain while minimizing the risk of contaminating one of the Kronian moons, which might harbour some fragile form of life. This final part of the mission became known as the *Grand Finale*. So it came to be that in April 2017, Cassini began a series of 22 orbits with periapses between the planet and its rings before finally plunging deep into the atmosphere and ultimately disintegrating on 15 September 2017.

The age and origin of Saturn’s rings has long been a subject of scientific discussion. While there is no definite consensus on their origin, with some scientists still advocating for a formation during the infancy of the solar system, this theory is difficult to reconcile with observations from our recent visits to Saturn. Already decades ago, Voyager observations suggested an influx of water ice particles from the rings along the magnetic field lines into the upper atmosphere, often referred to as *ring rain*<sup>1</sup> (Connerney, 1986; Connerney & Waite, 1984). This has since been confirmed by Cassini (Hamil et al., 2018; Hsu et al., 2018) and remote observations (O’Donoghue et al., 2013, 2017, 2019), signalling that the rings’ lifespan is finite, and we should perhaps consider ourselves lucky to be able to witness them in their present form before they eventually fade into the planet. If they were formed billions of years ago,

---

<sup>1</sup>*Ring snow* or *ring ice influx* might have been less alliterate but more suitable names as no liquid water droplets are found in this region of the solar system.



*Figure 1.2.* Artist's impression of Cassini between the rings and Saturn's atmosphere during the Grand Finale. Image credit: NASA/JPL-Caltech

this influx would have to be a recent (on astronomical timescales) development, as the material would have been depleted long ago at the observed rate (e.g., Connerney & Waite, 1984; Durisen & Estrada, 2023; Northrop & Connerney, 1987; O'Donoghue et al., 2019). Saturn seems to be literally devouring the rings, invoking its namesake in more than just size, as the titan Kronos is most notorious for eating his offspring to prevent them from usurping him.

Whilst closely related and further described in Chapter 3, the ring rain to mid-latitudes is not the main focus of the present thesis. Cassini revealed another, previously unexpected, connection between the innermost ring and Saturn's equatorial upper atmosphere: A substantial amount of ring material flows inwards from the D ring and subsequently shapes the composition and processes of the equatorial ionosphere just as much as ring rain shapes the mid-latitudes (e.g. Hsu et al., 2018; Mitchell et al., 2018; Moses et al., 2023; Perry et al., 2018; Wahlund et al., 2018; Waite et al., 2018). Developing a deeper understanding of the nature and effects of this influx on the plasma composition and chemistry in this region of Saturn's atmosphere has been the primary goal of my research conducted in the scope of this thesis.

The following Chapter 2 is intended to provide the basic theoretical background required for understanding the papers included in this thesis. Subsequently, Chapter 3 offers an overview of our understanding of Saturn and its rings prior to the Grand Finale. Chapter 4 summarizes key insights into Saturn's ionosphere gained during Cassini's Grand Finale to establish context for the included papers, with a focus on the connection to and effects of the ring influx. A brief overview of the relevant instrumentation is given in Chapter 5. The five papers included in this thesis are summarized in Chapter 6. Finally, Chapter 7 concludes this thesis with an outlook on the current state of our understanding of Saturn's ionosphere and its interaction with the rings, addressing major open questions and discussing opportunities for further research. A summary of the thesis in Swedish can be found in Chapter 8.

## 2. Some Basics of Planetary Ionospheres

The topic of planetary ionospheres offers much potential for an extensive description of the relevant theoretical background. For the purpose of conciseness, I will focus here only on the most important concepts that are required to understand the papers included in this thesis. This naturally omits many other relevant concepts and subjects in ionospheric physics, such as the coupling to the magnetosphere and the neutral atmosphere, currents, resistances, aurora, waves, and many others.

The most essential clue to answer the question of what makes that particular region of a planet's atmosphere the ionosphere is in the name. In this upper atmospheric layer, a significant fraction<sup>1</sup> of the atoms and molecules are ionized, which means that they carry an electric charge, forming a plasma. This ionization generally occurs via the impact of either an energetic photon or other particle, which transfers enough energy to the atom (or molecule) so that an electron is essentially "kicked out". This results in a free electron, leaving an atom (or molecule) with a positive charge, called a cation. The formation of negative ions (anions) via electron attachment or ion-pair formation is rarer and requires specific conditions to occur. For instance, in the D region of Earth's ionosphere the pressure is sufficiently high to allow for three-body reactions, for example  $e^- + O_2 + N_2 \longrightarrow O_2^- + N_2$  (Thomas & Bowman, 1985). In recent decades, a variety of anions have also been detected in extraterrestrial environments, such as in Titan's atmosphere, Enceladus' plume, and the coma of comet Halley (Coates et al., 2007, 2010; Millar et al., 2017).

These charged particles are subject to the electromagnetic force and thus behave very differently compared to the neutral atmosphere. They exhibit a collective behaviour that does not require collisions, as each electron and ion feels the presence of the other charged particles in its vicinity due to Coulomb interactions. This gives rise to unique effects in the broad subject of plasmas, such as the formation of current systems, and a multitude of plasma waves. A detailed description of plasma physics is outside the scope of this thesis, and the interested reader may wish to consult a relevant textbook for further insight (e.g. Baumjohann & Treumann, 1996; Cravens, 1997; Schunk & Nagy, 2009). Instead, I aim to provide a brief overview of the basic atmospheric physics and the concept of photochemistry, which describes the interaction of light with atmospheric constituents and the resulting changes of the latter.

---

<sup>1</sup>It should be noted that the fraction of charged to neutral particles in a planet's ionosphere can be as low as ~parts per million, and also varies significantly based on altitude, latitude, local time, season, solar activity, and many other factors.

## 2.1 Photochemistry

For a given volume of plasma, the temporal evolution of the density of any species is described by the respective continuity equation. To illustrate, we focus on electrons, for which it can be formulated as

$$\delta n_e / \delta t = Q - L - \text{div}(\mathbf{v}_e n_e), \quad (2.1)$$

with  $Q$  and  $L$  as the production and loss term, respectively. The last term,  $\text{div}(\mathbf{v}_e n_e)$ , describes the flux into (or out of) the volume via the electron drift velocity,  $\mathbf{v}_e$ , so the change in density due to transport. This can be set to zero if we assume an ionosphere in photochemical equilibrium (PCE). For PCE to apply, the chemical timescales (production and loss) must be sufficiently shorter than those of transport, meaning an electron or ion produced by photochemistry must be much more likely to be involved in a chemical reaction than to drift out of the volume of plasma. At its most basic, the plasma transport timescale can be obtained by comparing the scale height with the bulk plasma velocity (e.g. Moore et al., 2004). For Saturn's equatorial ionosphere, PCE is a reasonable assumption at altitudes  $\lesssim 2500$  km (Moore et al., 2018).

It should be noted that the species have different chemical lifetimes, which means that one species may be in PCE at a given altitude while others are not. A comparison between the local loss processes and the transport term determines whether PCE is applicable or not. The production and loss channels are unique for each species. For electrons the production term  $Q$  is mainly due to photoionization and the loss term  $L$  mainly due to recombination. A neutral particle can likewise be ionized by photons, impact of electrons, or charge-exchange reactions with other species and generally returns to neutral through recombination or further charge-exchange reactions.

A plasma is in overall charge equilibrium, which is referred to as quasi-neutrality. Generally, this means that the total densities of electrons and ions are equal (assuming singly charged ions), but this is not necessarily the case for a dusty plasma. Similar to a spacecraft, a dust grain immersed in a plasma will experience charging. The charge state of small grains can be estimated with formalisms such as the one devised by Draine and Sutin (1987). They calculate rate coefficients for electron- and ion attachment to grains as a function of grain size, charge state, and plasma temperature. Their formalism assumes spherical and conductive grains, and includes the fact that the electric field due to a charged particle approaching a grain causes electrostatic polarization of the latter.

## 2.2 Example of a simple photochemical model

To provide an example one-dimensional model encapsulating these concepts, we can look at the case of an atmosphere purely composed of atomic and

molecular hydrogen. First, we need the attenuated solar extreme ultraviolet (EUV) flux profile to calculate photoionization rates. For this purpose, we split the model into 1 km steps and calculate the photoabsorption for each step by multiplying the photoabsorption cross section of the neutral constituents with the attenuated flux from the superior step. This absorption is described by the exponential Beer-Lambert law

$$I(\lambda) = I_{\infty}(\lambda) \exp(-\tau(\lambda)), \quad (2.2)$$

with the attenuated flux at a given altitude step  $I(\lambda)$ , the flux at the top of the atmosphere<sup>1</sup>  $I_{\infty}(\lambda)$ , and the optical depth  $\tau(\lambda)$ . The equation for the latter, in the case of a vertical incident ray, is

$$\tau_{z_0}^v(\lambda) = \sum_j \sigma_j^a(\lambda) \int_{z_0}^{\infty} n_j(z) dz, \quad (2.3)$$

with the absorption cross sections of each species  $\sigma_j^a(\lambda)$  and the species' density height profiles  $n_j(z)$  integrated from the current altitude step  $z_0$  to infinity (Rees, 1989). The resulting profile can be analytically described by a Chapman function, but generally such calculations are done numerically. Naturally, the incident ray is generally not vertical to the atmosphere, and things become more complicated when considering a spherical atmosphere with variable incident angle. We can generally approximate the ionosphere as planar stratified layers, which results only in the addition of a sec  $\chi$  factor for  $\tau(\lambda)$  to describe the offset angle from zenith (see Rees, 1989).

Next we require a chemical reaction network. A simplified chemistry scheme for a hydrogen atmosphere is:



A variety of relevant reaction types are present even in this simple model, such as photoionization for Reactions 2.4–2.6 (dissociative in the latter case), radiative association for Reaction 2.7, charge exchange for Reaction 2.8, ion-neutral for Reaction 2.9, and dissociative recombination for Reactions 2.10–2.12. The above scheme naturally is oversimplified and applying it to Saturn's

<sup>1</sup>This can be obtained, for example, from TIMED/SEE measurements (Woods et al., 2005).

ionosphere does not capture the real conditions, as will be further discussed in Chapters 3 and 4 and the included papers.

Each reaction has its own reaction rate coefficient, and in the case of photoionization, the cross section of the respective species are multiplied with the EUV flux at the given altitude step. These rate coefficients are generally determined by laboratory experiments and can be conveniently retrieved from databases such as KIDA<sup>1</sup> and UMIST<sup>2</sup>. The relevant photo cross sections can likewise be found in, for example, the PHIDRATES<sup>3</sup> or the Leiden Observatory<sup>4</sup> databases. This together gives the momentary production and loss rates, but we are interested in the composition in a stable photochemical equilibrium. To evaluate this, the continuity equations for each species need to be iterated over many time steps. The required time until equilibrium is achieved varies based on factors such as complexity of the model or the inclusion of transport. The model output, shown in Figure 2.1, produces a characteristic ionization peak, whose shape is referred to as a Chapman layer. In more realistic cases, with complex chemical and transport processes, multiple of these layers may be present, or the shape may be more complex altogether. A comparison of our results with other models without ring influx, such as Atreya and Donahue (1975), shows broadly similar results around the peak.

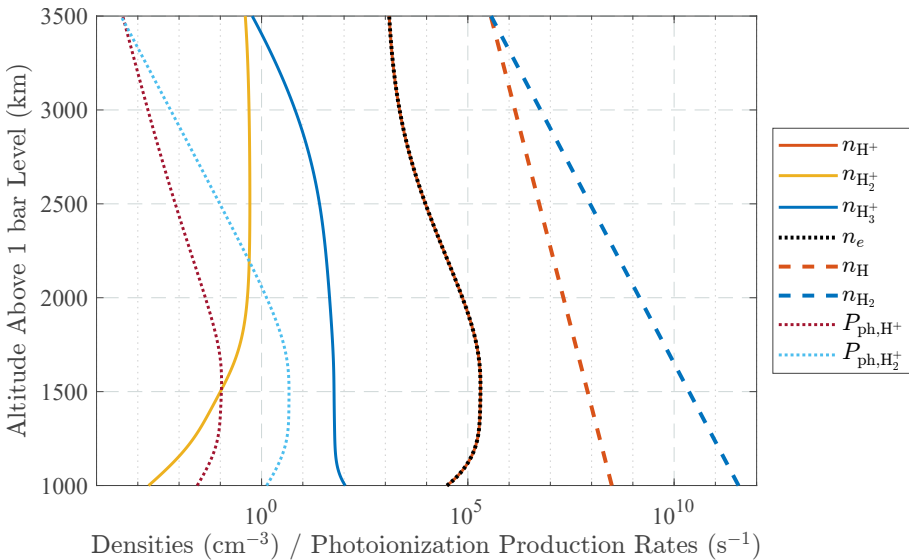


*Figure 2.1.* Model output for the case of a hydrogen atmosphere in photochemical equilibrium, showing the calculated ion, electron, and assumed neutral densities, as well as photoionization production rates.

<sup>1</sup><https://kida.astrochem-tools.org> (Wakelam et al., 2012)

<sup>2</sup><http://udfa.ajmarkwick.net> (McElroy et al., 2013)

<sup>3</sup><https://phidrates.space.swri.edu> (Huebner & Mukherjee, 2015)

<sup>4</sup><http://www.strw.leidenuniv.nl/~ewine/photo> (Heays et al., 2017)

### 3. Saturn and its Rings

As the second-largest planet in the solar system, Saturn is only surpassed in size by its big brother, Jupiter. On average, it orbits the Sun at a distance of 9.57 AU, completing a sidereal orbit in 10759 days or approximately 29.5 years. At this distance, Saturn receives only  $\sim 1\%$  of the solar irradiance compared to Earth. Lacking an observable surface, Saturn's shape is best described as an oblate spheroid. Its surface is by definition set at the level of 1 bar atmospheric pressure. Any altitudes specified in the following pages and included papers are given in relation to this level. Due to its fast rotation (10.7 hours) and compressible nature, Saturn has a polar radius of 54364 km and an equatorial radius of 60268 km, which gives it the distinction of being the most rotationally flattened planet. It is also noteworthy for having the lowest mean density, measuring just  $687 \text{ kg/m}^3$ , lower than that of water. This has led to the commonly used analogy that Saturn would float in a sufficiently sized bathtub. The gravitational implications of such a construction are at best brushed aside in this oversimplified thought experiment.

Saturn boasts an enormous number of satellites, with the current count as of the writing of this thesis being 146 moons with confirmed orbits (Sheppard et al., 2023). But this number will likely be higher at the time of reading and does not include all the tiny moonlets within the rings and objects with unconfirmed orbits. The seven major satellites, in particular, offer an exciting and vast field of study. Especially Saturn's biggest moon, Titan, and its icy sibling, Enceladus, are the focus of much current and future research. These moons may provide conditions conducive to primitive life, at least at certain stages during the Sun's lifespan. The interactions between Saturn's satellites, rings, magnetosphere, ionosphere, and atmosphere are incredibly complex and can offer much insight into the history of the solar system and fundamental space physics. An overview of the regions and interactions occurring within Saturn's magnetosphere is visualized in Figure 3.1.

#### 3.1 Pre-Cassini models and observations

Our understanding of Saturn before the Cassini mission was mainly based on observational data from the flybys of the Pioneer 11 and two Voyager probes in 1979–1981 and remote observations with telescopes. In models prior to these missions (e.g., Atreya & Donahue, 1975; McElroy, 1973), the major neutral ionospheric constituents were given as H, H<sub>2</sub>, He, and CH<sub>4</sub>. While these

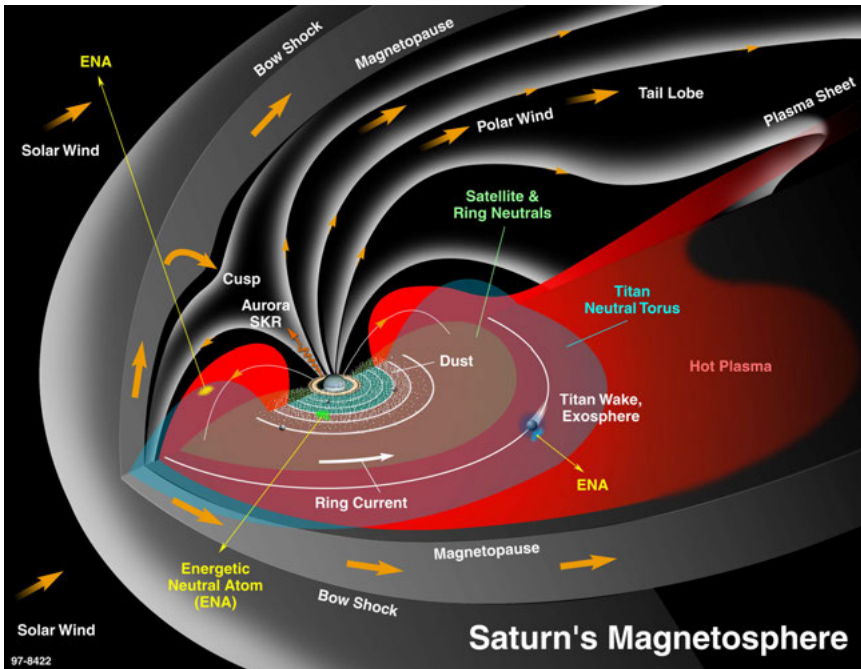


Figure 3.1. Illustration of the regions and processes within Saturn's magnetosphere. Figure reprinted from Krimigis et al. (2004) with permission from the publisher.

certainly are the dominant species, their mixing ratio profiles put forward at the time differ from our modern understanding, and many other neutral species that we now know to play an important role in the ionospheric chemistry are entirely missing. The only proposed ion species were  $\text{H}^+$ ,  $\text{H}_3^+$  and  $\text{HeH}^+$ , even near the ionospheric peak. While undoubtedly hard to predict at the time, we understand today that Saturn's ionosphere is rather more complex and species heavier than those listed prior are not only present, but also play a major role in the ionospheric chemistry. The inclusion of hydrocarbon ions by Capone et al. (1977) and study of the effects of varying eddy diffusion coefficient and temperature by Waite et al. (1979) increased the complexity of the models beyond these early stages.

Already before the first flybys, Atreya and Donahue (1975) suggested a potential connection between the rings and Saturn's upper atmosphere. This notion was strengthened when Pioneer and Voyager showed electron densities that were an order of magnitude lower than the model predictions. The dominant production channel for electrons in Saturn's ionosphere is the photoionization process  $\text{H}_2 + h\nu \longrightarrow \text{H}_2^+ + e^-$ . By far the most important loss channel for electrons is dissociative recombination with molecular ions, for which the rate coefficients are about five orders of magnitude larger than that for radiative association with atomic ions (e.g. Prasad & Huntress, 1980). Essentially, a mechanism was needed to convert atomic  $\text{H}^+$  ions into molecular

ions to reduce the electron density and reconcile the observations with model predictions. The two main suggestions were the ring rain theory proposed by Connerney and Waite (1984) and the charge exchange reaction



suggested by McElroy (1973), which is possible when  $\text{H}_2$  is in the fourth vibrational state or higher<sup>1</sup>. As one of the earliest models to describe the effects of both loss channels on the ionospheric chemistry, Majeed and McConnell (1991) concluded that both processes may play an important role in Saturn's ionosphere. Further elaborations on the ring rain theory can be found in Section 3.2. As for the loss channel via vibrationally excited  $\text{H}_2$ , it seems fair to state that this is somewhat of a loose parameter that models can tune. The reaction rate coefficient for Reaction 3.1 is based on estimates and the amount of vibrationally excited  $\text{H}_2$  in gas giants' ionospheres is poorly constrained. The main sources for vibrationally excited  $\text{H}_2$  are downward cascading from higher levels (fluorescence) that were excited by electron impact or energetic photons; electron impact excitation from the ground state; and dissociative recombination of  $\text{H}_3^+$  (Majeed et al., 1991). Moses and Bass (2000) stated this loss channel for  $\text{H}^+$  to be dominant compared to the loss from water influx, but based their assumed concentrations of vibrationally excited  $\text{H}_2$  on estimates by Majeed et al. (1991), which are themselves not well-constrained. The Cassini mission revealed that the influx of ring material indeed plays a major role, both in reducing  $\text{H}^+$  densities and also via enrichment of heavier species that increase the complexity of the ionospheric reaction network.

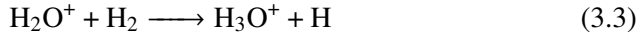
Prior to the arrival of Cassini, Moore et al. (2004) presented model results on the global variations within the ionosphere after coupling to a global circulation model of the thermosphere (Müller-Wodarg et al., 2006) and the effects of ring shadowing. They determined that photochemical equilibrium is applicable over a large range of altitudes, between  $\sim 1000$ – $2300$  km. The homopause is estimated to be located near  $1000$  km, and above  $\sim 2300$  km the chemical timescale of electron-ion recombination exceeds that for ion-neutral diffusion and thus transport processes start to dominate<sup>2</sup>. The intermediate region between these two levels is also the primary focus of the papers included in this thesis. The basic notion of an ionosphere dominated by hydrogen and helium and their respective ions has not necessarily changed since the Voyager era. In contrast, the presence, mixing ratios and exact composition of heavier species were much less certain and our understanding in this regard has evolved significantly due to the insights Cassini provided. The recent observations from Cassini's Grand Finale and the development of newer ionospheric models, which include these discoveries, are further discussed in the following Chapter 4.

<sup>1</sup>Molecules possess more degrees of freedom than atoms and exhibit additional quantum states related to the vibration of the bonded atoms and the rotation around their centre of mass.

<sup>2</sup>For the proximal orbits near the equator this is closer to  $2500$  km.

## 3.2 Ring rain to mid-latitudes

As described above, ring rain is one of the main explanations for the lower than expected electron densities in Saturn's ionosphere. The influx of water ice particles provides an efficient loss channel for electrons due to the enrichment of molecular ions with much higher recombination rate coefficients than for atomic hydrogen ions. The fundamental chemical reactions, as outlined by Connerney and Waite (1984), describing this process are:



Atomic hydrogen ions are converted to molecular ions via Reactions 3.2 and 3.3, which then efficiently reduce the electron density via Reactions 3.4–3.6. Whereas the exact composition of the inflowing particles was inferred (rather than measured in-situ) prior to arrival of Cassini, the effect of most suggested species remains similar: Ultimately, a reduction in atomic ions and subsequently also a reduction in electron densities due to the higher concentration of molecular ions with higher recombination rate coefficients. It should be noted that the influx does not necessarily have to be in the form of  $\text{H}_2\text{O}$ , as hydroxyl radicals (OH) are quickly converted to  $\text{H}_2\text{O}$  via Reaction 3.7. The same applies to any water group ions via other photochemical reactions (e.g., Moses & Bass, 2000), bringing us back to the above equations for inflow of any water group species. Hsu et al. (2018) also determined a substantial relative abundance of silicates in Cassini Cosmic Dust Analyzer (CDA) data for the ring rain to these mid-latitudes, notably higher than that of the main rings itself, pointing toward sputtering by cosmic dust as a major source for the excess fraction (Kempf et al., 2023).

## 3.3 Revelations from Cassini prior to the Grand Finale

With the arrival of Cassini in 2004 began a period of constant new insights into the Kronian system for over a decade. While the term "revolutionized" is often used as hyperbole, Cassini indeed transformed our understanding of the Kronian system, revealing many complex interactions and phenomena during its 292 orbits around Saturn (e.g., Spilker, 2019). Dougherty et al. (2009) provide a comprehensive overview over the first years of Cassini's discoveries, and Baines et al. (2018) do the same for the latter half of its mission around Saturn prior to the Grand Finale. In this thesis and the included papers, I focus

almost exclusively on the low-latitude ionosphere and thus not only exclude high-latitude phenomena, such as aurora, but also the complex magnetosphere-ionosphere coupling and the far-reaching interaction with the main rings and beyond (e.g. Galand et al., 2011; Müller-Wodarg et al., 2012). The view to lower altitudes likewise reveals an active and complex research environment. The recent advances in our understanding of, for example, the structure and chemistry in the deeper reaches of Saturn’s atmosphere (e.g., Moses et al., 2023; Yelle et al., 2018), its interior and variations in gravitational potential (e.g., Iess et al., 2019), and Saturn’s circulation and weather patterns (e.g., Brown et al., 2020; Galanti et al., 2019; Müller-Wodarg et al., 2019) are far too complex to cover here. The two books mentioned above and the respective chapters within may serve as a starting point for any reader interested in these topics.

Purely focusing on the topics most relevant for this thesis, Cassini’s many years around Saturn prior to the Grand Finale still provided us an unprecedentedly close view of the inner ring regions and Saturn’s ionosphere. Some of these discoveries include:

- The first radio occultation measurements exhibited significant dawn-dusk and orbit-to-orbit variability, suggesting an influx of water around the equator (Moore et al., 2006; Nagy et al., 2006).
- The ionization by photoelectrons was shown to become a significant production process by Galand et al. (2009) at altitudes around and below the main ionospheric peaks.
- Regions dominated by hydrocarbon ions are predicted to be present at lower ionospheric altitudes (600–1000 km) by Kim et al. (2014).
- The D ring has significantly changed since the Voyager flybys and shows variable structures, one of which may be the result of a cometary impact (Hedman et al., 2007).
- Saturn’s ionosphere is highly variable on both small and large scales, which is likely linked to variations in ring influx and energy transfer via gravity waves from the neutral atmosphere below (Barrow & Matcheva, 2013; Kliore et al., 2009; Matcheva & Barrow, 2012; Moore et al., 2010; Moses & Bass, 2000).

### 3.4 Saturn’s rings

As we are discussing the connection between the ionosphere and Saturn’s rings, it is worth briefly summarizing the main structure and attributes of the latter. The rings of Saturn are, somewhat inconveniently, not alphabetically named with increasing distance from the planet, but rather chronologically by their first discovery date. Thus, we start with the faint D ring as the innermost structure, followed by the C, B and A rings. These three are often referred to as

the main rings, as they are the brightest and thus were discovered first. Just a bit further out lies the very narrow F ring, and after a larger gap the faint G and E rings conclude the alphabetical journey. The E ring extends far outwards to the orbit of Titan. It is not the outermost ring though – this epithet belongs to the very faint Phoebe ring discovered by Verbiscer et al. (2009). An overview of the rings is shown in Figure 3.2.

They are separated and shaped by a multitude of structures, some of which are large enough to be easily visible, while others are subtle variations in ring particle density (Tiscareno et al., 2019). These structures are generally the results of gravitational interactions between Saturn and its moons, and many of them can be attributed to resonances from individual satellites. For example, the A and B rings are separated by the Cassini Division, discovered by the eponymous Italian scientist in 1675. This gap is caused by an orbital resonance with the moon Mimas. Another gap and its causative moon are shown in Figure 3.3. More subtle examples of such effects are the tiny substructures called ringlets and plateaus in the C ring, which we discuss further in Paper III. A comprehensive overview of Saturn’s rings is given by Colwell et al. (2009), Cuzzi et al. (2018), and Tiscareno et al. (2019).

Besides their structural complexity, Saturn’s rings also vary in composition. Comparing the connection of different parts of Saturn’s ionosphere to the rings involves tracing the infalling particles to their origin, and generally particles from different regions of the ring system vary in composition and size. These differences can be seen not only when comparing the larger structures, but even within individual ring substructures (e.g., Colwell et al., 2018; Jerousek et al., 2020). Broadly speaking, the rings are mainly made up of water ice grains, but a variety of other substances can also be found within (Zhang et al., 2017a,b). To complicate things further, both structure and composition of the rings evolve over time due to micrometeoroid bombardment and changes caused by solar UV radiation (Estrada et al., 2015; Kempf et al., 2023). This becomes especially relevant when studying their origin and lifetime (e.g. Estrada & Durisen, 2023). Notably, even on human timescales, the D ring has undergone significant changes since the Voyager flybys, including the disappearance or movement of some substructures (e.g., Cuzzi et al., 2009; Hedman et al., 2007). The rings possess their own ionosphere, with Enceladus as a major source and transport in the magnetosphere both in- and outward (Persoon et al., 2005, 2013; Tokar et al., 2005), and the E ring has been observed to interact collectively with Saturn’s plasma disk (Wahlund et al., 2009).

Whereas the ring rain described in Section 3.2 primarily originates in the A, B, and C rings and precipitates along the magnetic field lines, this is not the primary origin of the ring influx studied in Papers I, II and IV. The equatorial ionosphere is directly connected to the D ring, which extends from 65,000–74,000 km from Saturn’s centre (Hedman et al., 2007), and it is worth discussing this particular ring in a bit more detail. Prior to Cassini, very little about the D ring’s finer details was known. Due to its faintness, it is

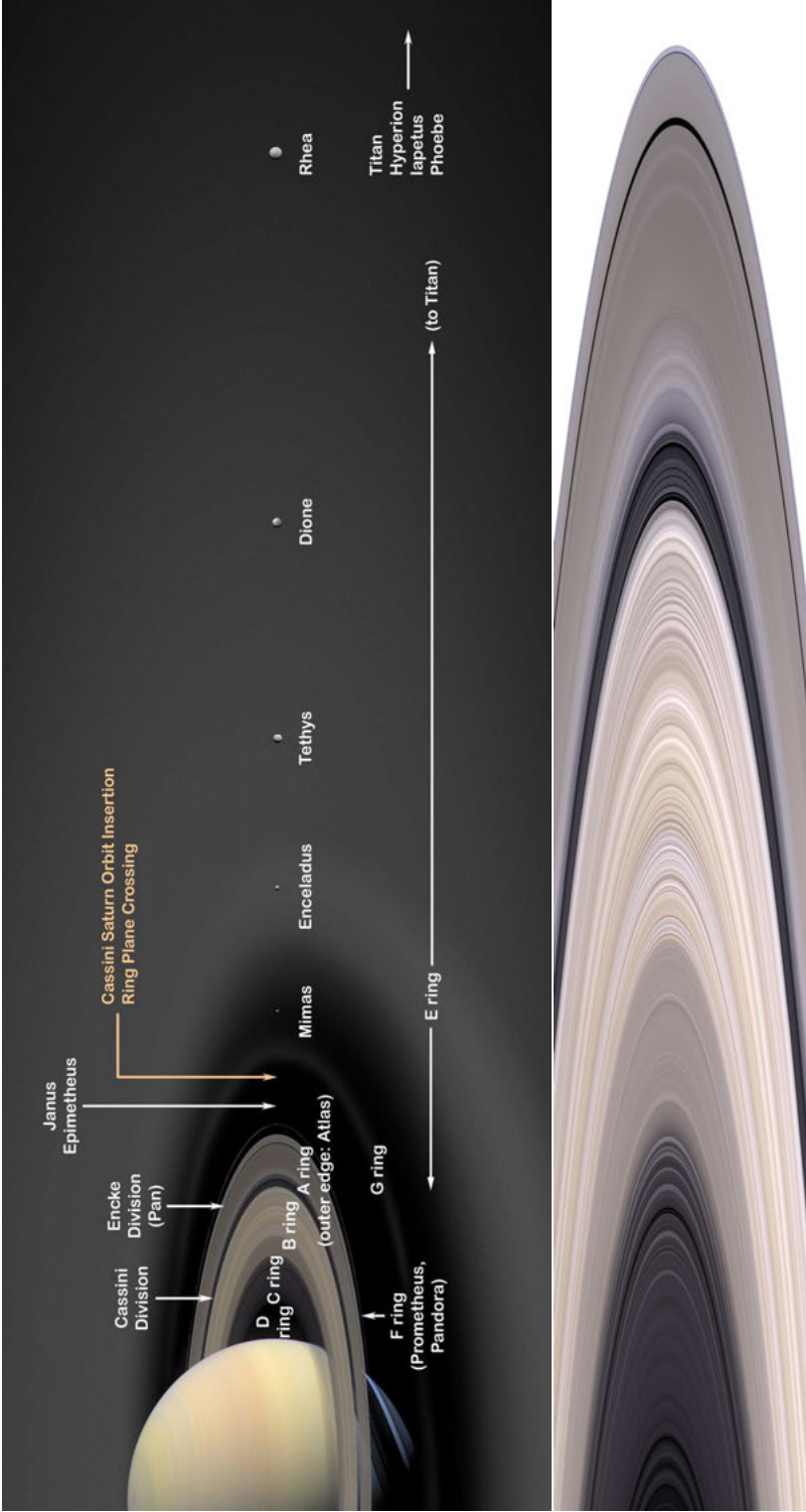
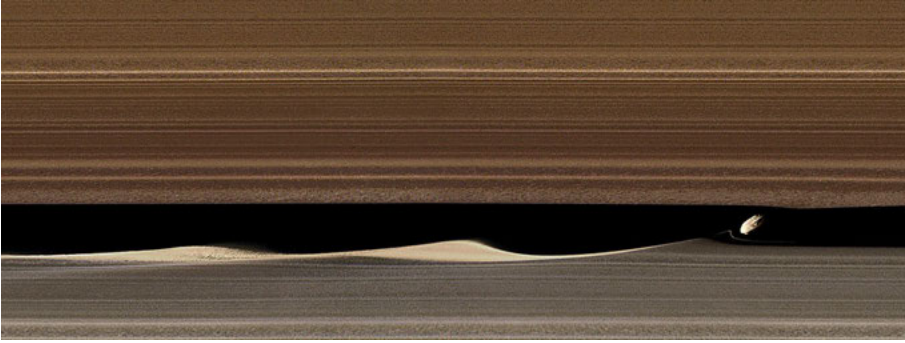


Figure 3.2. Top: Artist's impression of Saturn's moons and rings with their respective labels. Bottom: Cassini Imaging Science System (ISS) mosaic of the D, C, B, and A rings, from left to right. Image credit: NASA/JPL/Space Science Institute



*Figure 3.3.* Image mosaic of the moon Daphnis shaping the Keeler gap in Saturn's A ring. Image credit: NASA/JPL-Caltech/Space Science Institute

difficult to observe with telescopes and the Voyager flybys provided the last up-close images. Over the duration of the Cassini mission, many new details about this ring and its connection to the ionosphere were revealed. It exhibits variations in both composition and its substructures over short timescales of a few years (Hedman et al., 2007). This suggests that the influx of ring material may likewise show significant temporal variability, which in turn changes the equatorial ionospheric composition. Hedman et al. (2009) suggest that some observed perturbations in the D ring might not be caused by gravitational interaction, and are instead connected to periodic signals in Saturn's radio emissions. The D ring contains a few narrow ringlets (e.g., Horányi et al., 2009), some of which are proposed sources of small infalling D ring particles (1–10  $\mu\text{m}$ ) detected toward the inner edge of the ring (Cuzzi et al., 2009). Overall, typical grain sizes within the D ring are between 1–100  $\mu\text{m}$  (Hedman et al., 2007).

Cassini's measurements of the rings and the rate of their disappearance into the atmosphere also allows an estimation of upper limits for their lifetimes, and thus origin. Comparisons of CDA cosmic dust measurements, ring composition and mass, and ballistic transport models collectively suggest that the rings are only a few hundred million years old, much younger than their giant (Durisen & Estrada, 2023; Estrada & Durisen, 2023; Jess et al., 2019; Kempf et al., 2023). Teodoro et al. (2023) reason that they might have been born a few hundred million years ago in a collision of two icy moons, whereas Wisdom et al. (2022) propose that they might have originated in a moon migrating too close to the giant, eventually being ripped apart by the enormous tidal forces. Thus, Cassini's journey also provided a window into the history of our solar system, transporting us back to a time when life on Earth just began to truly flourish.

## 4. Insights from Cassini's Grand Finale

*We are the representatives of the cosmos; we are an example of what hydrogen atoms can do, given 15 billion years of cosmic evolution.*

Carl Sagan

This chapter is meant to give a concise overview of some major results from the Grand Finale and provide a background for the papers included in this thesis. A graphical abstract of my main research foci is shown in Figure 4.5. There are many other revelations from Cassini's Grand Finale that cannot be covered here, and the included selection of references might serve to further inform on whichever points the reader finds most intriguing. I will start with a description of the proximal orbits for context in the following section.

### 4.1 Proximal orbits

On 22 April 2017, Cassini began the final phase of its mission, which culminated with its destruction in the atmosphere of Saturn on 15 September. The 22 full orbits (#271–292) and the final plunge (#293) which constitute the Grand Finale are high-inclination orbits with periapses at latitudes of approximately  $-5^\circ$  ( $\sim 10^\circ$  for the final plunge) and altitudes down to  $\sim 1700$  km, approximately aligned north-south and crossing the subsolar point around closest approach. The time between subsequent periapses was about 6.5 days. This was the first time the region between Saturn's atmosphere and its rings was sampled in



*Figure 4.1.* Artist's impression of Cassini during the Grand Finale. Image credit: NASA/JPL-Caltech

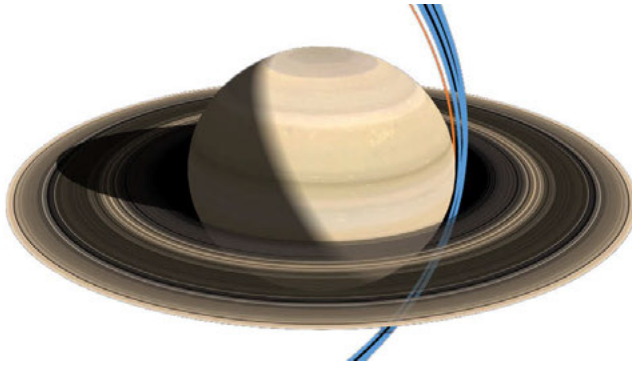


*Figure 4.2.* Illustration of Cassini’s Grand Finale orbits (blue) and the final plunge (orange). Image credit: NASA/JPL-Caltech/Erick Sturm

situ. An illustration of the proximal orbits is shown in Figure 4.2. Particularly orbits 283, 287, 288 and 292 are relevant for the included papers, as light ion densities were sampled during these orbits, and the latter two reached altitudes well below 2500 km at periapsis, where photochemical equilibrium applies (Moore et al., 2018). These orbits are shown in Figure 4.3.

## 4.2 Ring influx around the equatorial plane

Compared to the relatively old theory of ring rain along the magnetic field lines described above, the Grand Finale revealed an unexpected new connection between Saturn and its rings. During Cassini’s dives between the innermost D ring and the top of Saturn’s atmosphere, a very substantial inward flux of ring material was detected around the equatorial latitudes of the ring plane, which is discussed below. While interplanetary dust is present in the atmospheres of all giant planets (e.g., Poppe, 2016), this flux is too low to explain the observational results from Saturn even prior to the Grand Finale. The connection between the rings and the ionosphere had long been theorized upon, but Cassini was the first mission to sample the dust grains themselves and provide measurements of their actual composition not purely based on model constraints. This resulted in many new insights, some of which are highlighted below and visualized in Figure 4.6.

For an initial overview, we consider the results by Waite et al. (2018), who measured the composition of the upper equatorial atmosphere during the Grand Finale with the Ion and Neutral Mass Spectrometer (INMS, see Section 5.2). Besides the expected signal for molecular hydrogen and helium, other abundant neutral species include water, organics, methane and a signal at a mass of 28 Da. This could be either CO, N<sub>2</sub> or C<sub>2</sub>H<sub>4</sub>. Their estimated fluxes for the ring material are between 4800–45,000 kg s<sup>-1</sup> in a region of 8° around

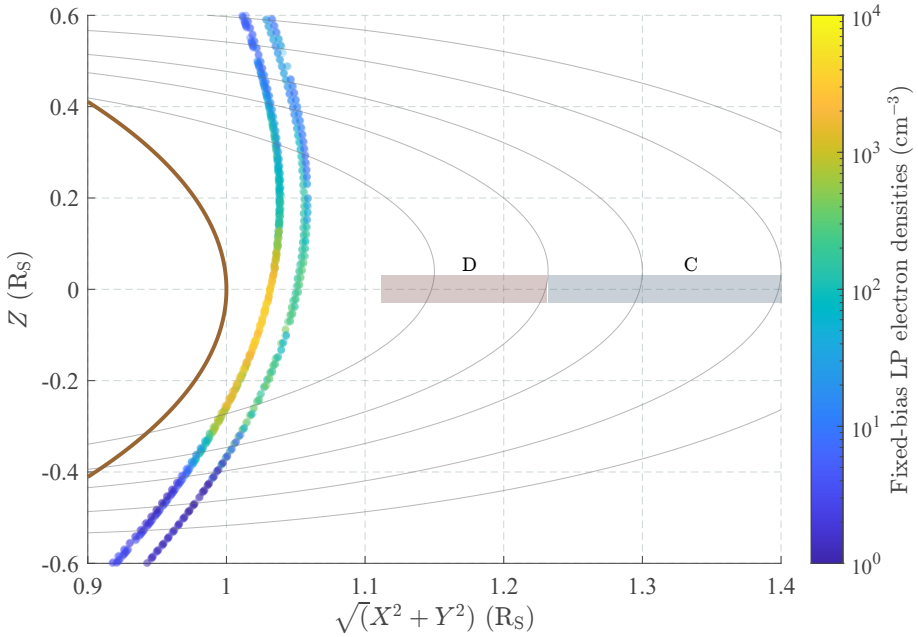


Figure 4.3. Proximal orbits 283, 287, 288, and 292 shown in planetocentric equatorial coordinates, with the magnetic field lines mapping to the ring plane, based on the magnetic field model by Burton et al. (2010). Fixed-bias LP electron densities are shown on a logarithmic colour scale. Saturn’s 1-bar level is shown as a brown line.  $R_S \equiv$  Saturn’s equatorial radius = 60268 km

the equator. Such an influx of heavy species will significantly alter the expected ionospheric chemistry compared to the simpler models described in Chapters 2 and 3. They suggest that due to the tenuous nature of the D ring, a constant supply from the C ring is likely required to sustain these fluxes. In addition to these INMS measurements, a population of nanometer-sized grains was directly sampled with the Magnetospheric Imaging Instrument (MIMI) and analysed by Mitchell et al. (2018). Their analysis showed a large influx of tiny dust grains (here referred to as nanograins) with masses of 8000–40,000 Da and corresponding radii of 1–3 nm. Hsu et al. (2018) measured the makeup of larger dust particles inward of the D ring with the cosmic dust analyzer (CDA). Their results around the equator show grains which are mostly a few tens of nanometres in radius and composed mainly of water ice and some silicates. The fraction of silicates increases towards mid-latitudes, far beyond that of the rings itself, which suggests micrometeoroid bombardment as a source (e.g. Kempf et al., 2023). The effects of this influx of ring material from the D ring on the ionospheric composition are the focus of Papers I, II, IV and V.

As predicted in model results by Moore et al. (2004) and confirmed by various observational studies based on Cassini data, the rings affect the ionosphere beyond supplying material – they also absorb solar radiation and thus provide a spatial variation in solar irradiance, which manifests itself in lower photoion-

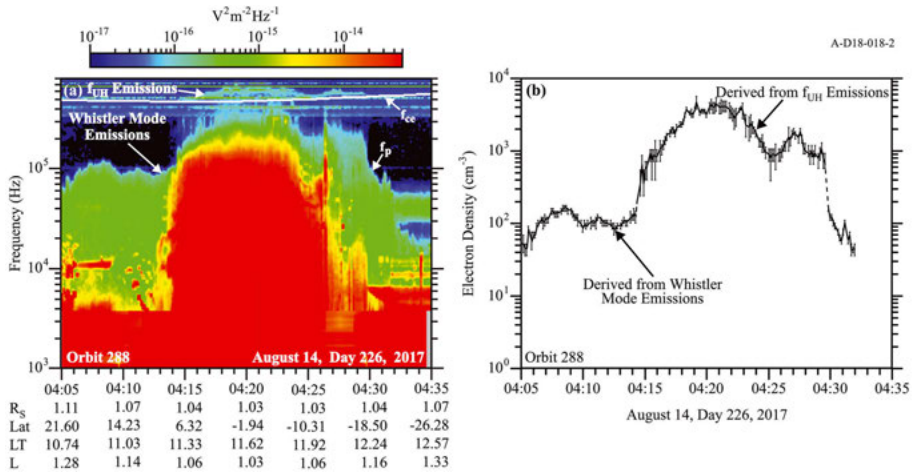


Figure 4.4. Left: Radio and Plasma Wave Science (RPWS) observations during orbit 288. Right: Derived electron densities (see further Section 5.1). Figure reprinted from Persoon et al. (2019) with permission from the publisher.

ization rates. Clear decreases in electron and ion densities within the shadowed regions are shown by Hadid et al. (2018), Wahlund et al. (2018), and Waite et al. (2018). Whereas the  $\text{H}_3^+$  densities decline rapidly in the shadowed areas, the  $\text{H}^+$  densities decrease somewhat slower, which indicates transport of  $\text{H}^+$  into these regions (Hadid et al., 2018). Ionospheric effects of ring shadowing are also the main focus of Paper III included in this thesis. Morooka et al. (2019) report on high levels of electron depletion near closest approach for the Grand Finale orbits, as well as unexpectedly high electron temperatures. The electron densities exhibit a north/south asymmetry and vary significantly between orbits, as results by Hadid et al. (2019) show. These variations appear to be stronger in the southern hemisphere, and the respective latitudes are connected to the D ring via the planetary magnetic field. Signatures of whistler mode emissions have been observed in this region by Sulaiman et al. (2017).

In the following, I will briefly list some other relevant studies which are discussing this region. Chadney et al. (2022) investigate the energy input from energetic photons and electrons into Saturn's equatorial atmosphere, and assess the relative importance of electron impact ionization. Hamil et al. (2018) describe how and where ice grains vaporize in Saturn's ionosphere. At assumed initial grain sizes of 1–10 nm, most of their energy is estimated to be deposited between 1700–1900 km. The grains are shown to only significantly vaporize if their initial velocity is  $>20$  km/s, which then permits adding water vapour to the upper atmosphere. The RPWS wave-derived electron densities, shown in Figure 4.4, are compiled by Persoon et al. (2019). Their results, along with the analysis by Hadid et al. (2019), show an ionosphere with three distinct layers. Above 4500 km, the plasma is almost exclusively composed of  $\text{H}^+$  (and electrons) and convective transfer is dominant, whereas below

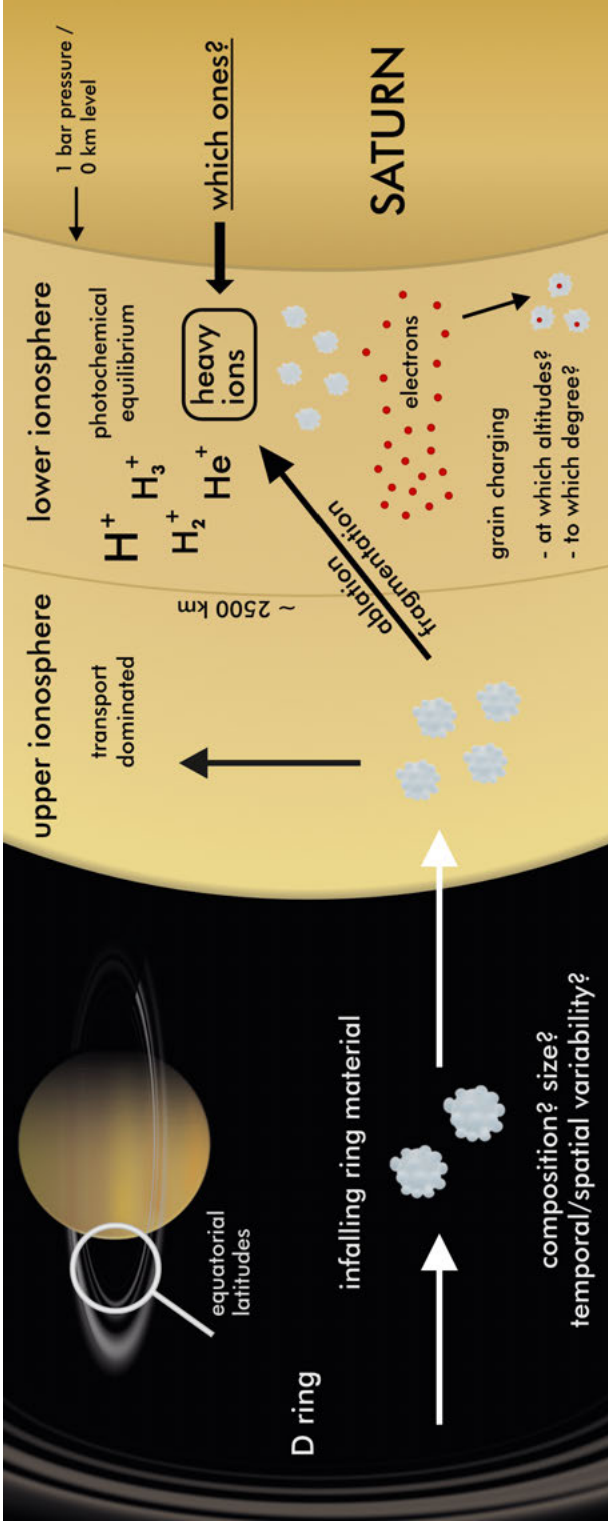


Figure 4.5. Graphical abstract of the main research foci of the papers included in this thesis.

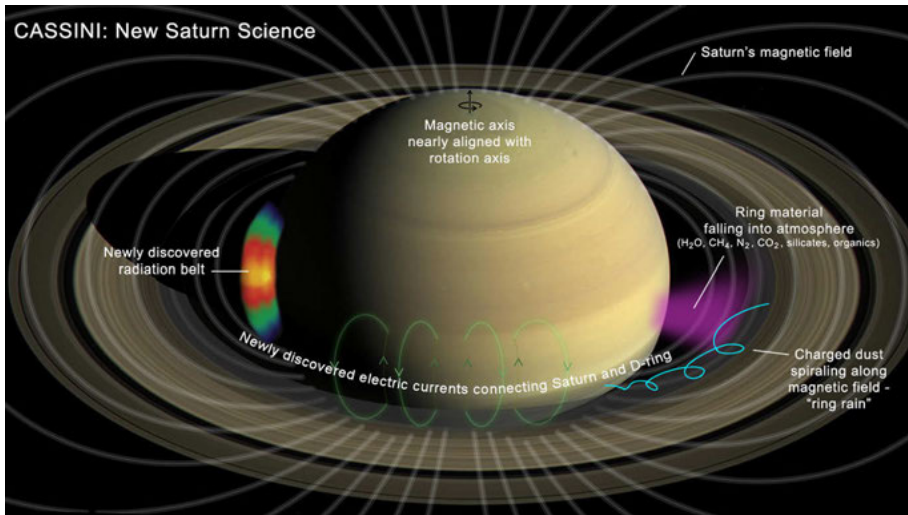


Figure 4.6. Illustration of new insights from Cassini's Grand Finale, depicting the coupling and environment between the inner rings and Saturn's ionosphere. Image credit: NASA/JPL-Caltech

2500 km the chemical timescales are sufficiently short for PCE to apply. The region between these levels can be described as a diffusive and highly variable layer where transport dominates over chemical processes and electron densities decrease exponentially. And lastly, emissions from a radiation belt between the D ring and the equatorial atmosphere were detected by Krimigis et al. (2005), which was then probed in situ during the Grand Finale (Kollmann et al., 2018; Roussos et al., 2018).

### 4.3 New models of Saturn's ionosphere

A study by Moore et al. (2018) incorporates the Grand Finale observations into a comprehensive effort to model the effect of the ring influx on Saturn's ionosphere. In Figure 4.7, their model results, based on measurements from orbit 288, are presented. Panels (a)–(c) display ionospheric profiles based on selecting a different single species for the mass 28 Da signal reported by Waite et al. (2018). In all three cases, the model predicts the presence of numerous heavier ion species in significant concentrations. These include various water group and complex hydrocarbon ions, especially at lower ionospheric altitudes. Based on estimates by Perry et al. (2018), they select a mixing ratio of 28% C<sub>2</sub>H<sub>4</sub>, and 36% for both of N<sub>2</sub> and CO as the 28 Da species. A comparison between their model results and Cassini INMS light ion data for orbits 288 and 292 are shown in Figure 4.8. They note a requirement to increase the measured EUV flux, which serves as model input, to match the modelled H<sub>2</sub><sup>+</sup> densities with those measured by INMS. Furthermore, the modelled H<sub>3</sub><sup>+</sup> densities ex-

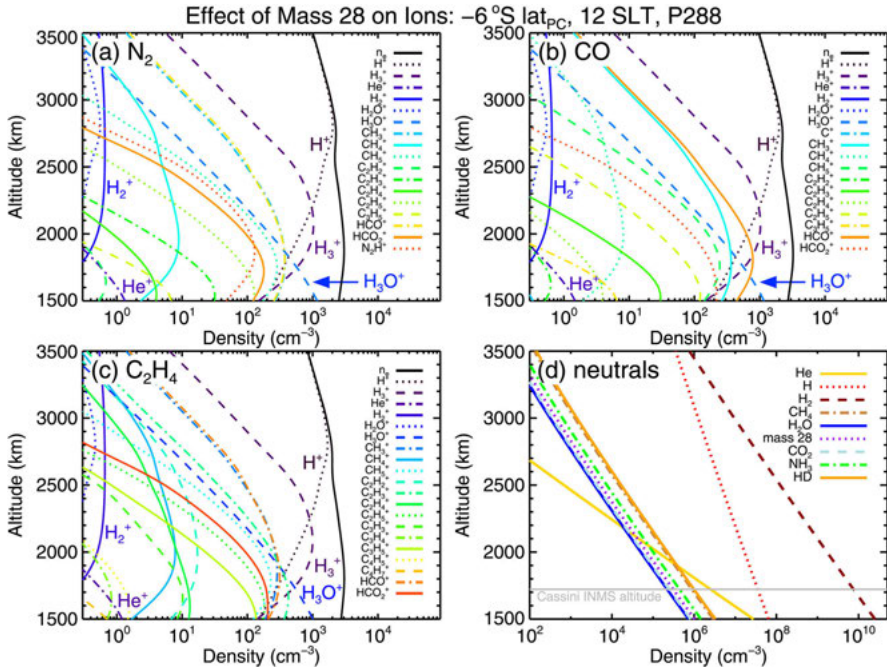


Figure 4.7. Model results for orbit 288 by Moore et al. (2018), who incorporate the detections of infalling dust grains and study how their composition affects the ionospheric chemistry. In panels (a)–(c), the varying model predictions for different species selected as the 28 Da signal described by Waite et al. (2018) are shown. The neutral model input is shown in panel (d). Figure reprinted from Moore et al. (2018) with permission from the publisher.

ceed, and the modelled  $\text{H}^+$  densities fall short of the measured densities around the closest approach. As a result, they stipulate a loss mechanism involving species that are reactive with  $\text{H}_3^+$  without affecting  $\text{H}^+$ .

This is expanded upon by Cravens et al. (2019b), who empirically calculate the mixing ratios of two types of species, denoted M and R, to account for the observed concentrations of  $\text{H}^+$  and  $\text{H}_3^+$ . M-type species (such as  $\text{H}_2\text{O}$ ,  $\text{CH}_4$ , and  $\text{NH}_3$ ) are reactive with both  $\text{H}^+$  and  $\text{H}_3^+$ , whereas R-type species (such as  $\text{CO}$  or  $\text{N}_2$ ) only meaningfully contribute to the loss of the latter. Their analysis suggests that to explain the observed  $\text{H}^+$  and  $\text{H}_3^+$  densities, the lower equatorial ionosphere is likely strongly influenced by these heavy neutral molecular species, with an estimated volume mixing ratio of  $\sim 100$  ppm. An estimate of their latitudinal profile points to a dominance of R-type species around the equator, whereas M-type species are more abundant at slightly more poleward latitudes. Understanding the abundance, nature, and effects of these heavier neutrals and the resulting ion species was a primary focus of the studies included in this thesis, and these questions are further investigated in Papers II and IV.

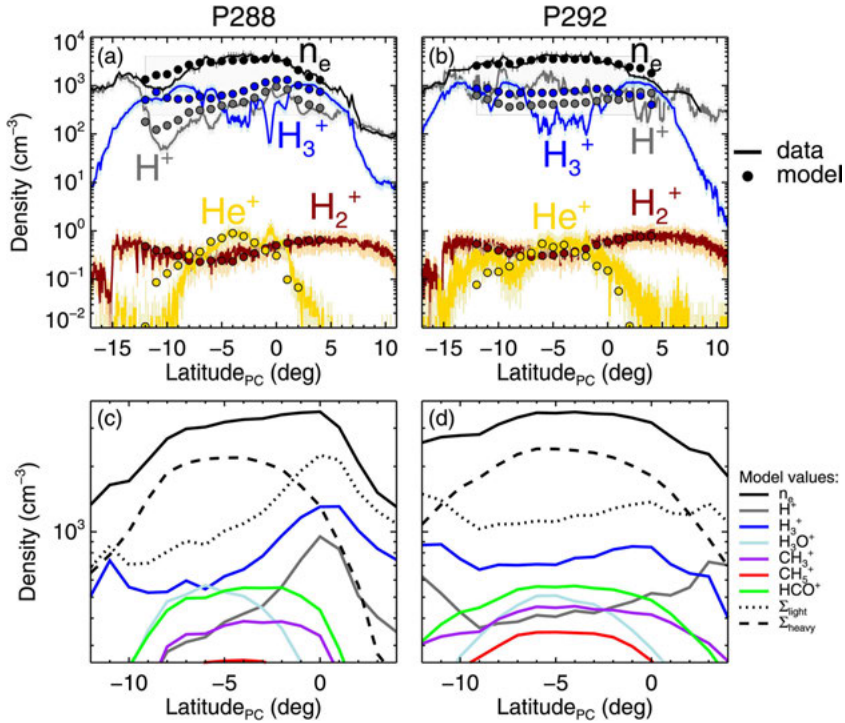


Figure 4.8. Model results by Moore et al. (2018) for orbits 288 and 292 compared to Cassini data. The two lower panels show modelled plasma densities near closest approach, which is the region marked by a grey box in the upper panels. Figure reprinted from Moore et al. (2018) with permission from the publisher.

A comprehensive new model by Moses et al. (2023) expands upon the model by Moore et al. (2018) by including a more complex chemical reaction network, expansion to lower altitudes and investigation of the effects of variations in the ring influx and its distribution. It should be noted that the effects of grain charging, such as discussed in Paper II, are not included in this model. Their model considers and compares a variety of cases, differing by the model input data, assumptions on distribution of the ring material, and how much of it actually affects the ionospheric chemistry. They present a conundrum with two suggested explanations, which are worth highlighting here: To explain the absence of observations of the effects such a large influx of ring material would have on the stratospheric chemistry, they suggest that either 1) only the most volatile molecules that were visible in the INMS mass spectra ( $\text{N}_2$ ,  $\text{CO}$ , and  $\text{CH}_4$ ) significantly ablate in the ionosphere to enter the gas phase and partake in the plasma chemistry, and most of the other detected species in the INMS data result from impact fragmentation of grains, or 2) the ring influx detected during the Grand Finale is a very recent phenomenon and thus was not observed earlier during the mission. We will further discuss the first option in the context of Paper IV.

## 5. Instrumentation

For the papers included in this thesis, data from two instrument packages onboard Cassini were used: The Radio and Plasma Wave Science (RPWS) instrument suite and the Ion and Neutral Mass Spectrometer (INMS). A non-exhaustive overview of these instruments is given below, and the references within provide more in-depth descriptions. Other relevant instrumentation for studying the plasma environment around Saturn were the Cassini Plasma Spectrometer (CAPS, Young et al., 2004), which unfortunately was non-operational by the time of the Grand Finale, and surely would have otherwise provided a deeper insight into the ionospheric plasma in conjunction with the operational instruments, the Magnetospheric Imaging Instrument (MIMI, Krimigis et al., 2004), and the Cosmic Dust Analyzer (CDA, Srama et al., 2004).

The instruments that were measuring until Cassini's disintegration in the final plunge are labelled in Figure 5.1. An artist's sketch of the entire Cassini-Huygens spacecraft with labelled components is shown in Figure 5.2. Apart from the instrumentation onboard Cassini, solar EUV data gathered by the Solar EUV Experiment (SEE, Woods et al., 2005) onboard NASA's Thermosphere Ionosphere Mesosphere Energetics and Dynamics (TIMED) mission were utilized in the included papers for photochemical modelling of Saturn's ionosphere.

### 5.1 Radio and Plasma Wave Science (RPWS)

No serious planetary mission targeting space plasma environments is complete without a way to measure radio emissions, plasma waves and electron densities. As the name implies, for the Cassini mission this was the task of the Radio and Plasma Wave Science (RPWS) instrument suite, which is described in detail by Gurnett et al. (2004). Its main constituents were the electric field sensor (three 10 m antenna elements measuring fields in a frequency band from 1 Hz to 16 MHz), the magnetic field sensor (three orthogonal search coil magnetic antennas detecting fields between 1 Hz to 12 kHz in frequency range, see Dougherty et al., 2004) and the Langmuir probe (LP), which measured electron and ion densities and temperatures.

Compared to the instruments onboard the Voyager probes, the RPWS instruments offered much-improved sensitivity, dynamic range and the ability to directionally constrain observed remote emissions. The inclusion of a Langmuir probe also enabled direct in-situ sampling of the local plasma environment.

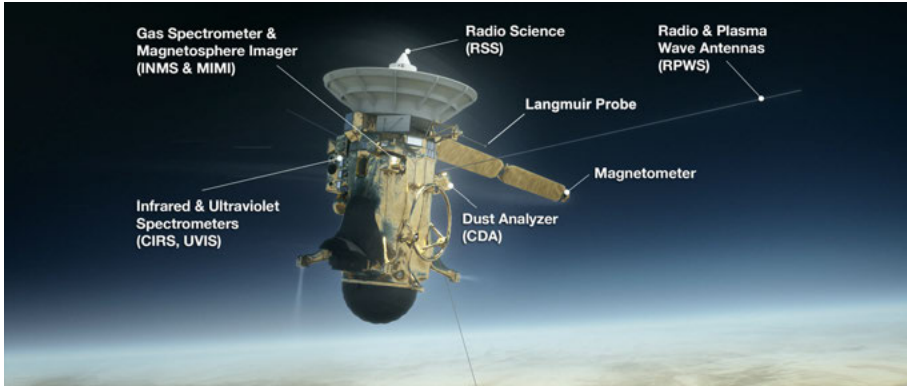


Figure 5.1. Artist's impression of Cassini during the final plunge. The labelled instruments were measuring Saturn's upper atmosphere until the end. Image credit: NASA/JPL-Caltech

Of particular relevance for this thesis, other than the LP described below, is the derivation of electron densities from the RPWS radio wave observations, namely those of whistler mode and narrowband upper hybrid frequency emissions, as described by Persoon et al. (2019). For the former, their upper cutoff is due to resonance at the electron plasma frequency  $f_{pe}$  in low-density regions where  $f_{pe}$  is less than the electron cyclotron frequency  $f_{ce}$ , visible as the upper edge of the broad green region in the left panel of Figure 4.4. The electron density in  $\text{cm}^{-3}$  can be derived easily from this frequency in Hz with the commonly used relation

$$f_{pe} = 8980\sqrt{n_e}. \quad (5.1)$$

In high-density regions, such as those encountered during the proximal orbits,  $f_{pe} > f_{ce}$ , and thus the whistler mode emissions are damped and not driven into resonance. Instead, the electron density can be obtained from upper hybrid emissions observed in this region. To accomplish this, the plasma frequency is derived from the upper hybrid frequency  $f_{UH}$  with the relation  $f_{UH}^2 = f_{pe}^2 + f_{ce}^2$ , with all frequencies in Hz, and subsequently the electron density via Equation 5.1. The cyclotron frequency in Hz can be obtained from magnetic field measurements,  $f_{ce} = 28 B$ , with  $B$  in nT (Gurnett et al., 2005). Compared to the LP, the RPWS wave observations sample a larger volume around the spacecraft and thus provide a view of the unperturbed plasma.

### 5.1.1 Langmuir probe (LP)

The Cassini LP was a titanium sphere of 5 cm diameter, coated with titanium nitride. It was mounted on a 0.8 m hinged boom folding outward for deployment. The entire assembly is shown in Figure 5.3. Plasma densities and temperatures measured by the LP were used for the analyses presented in the

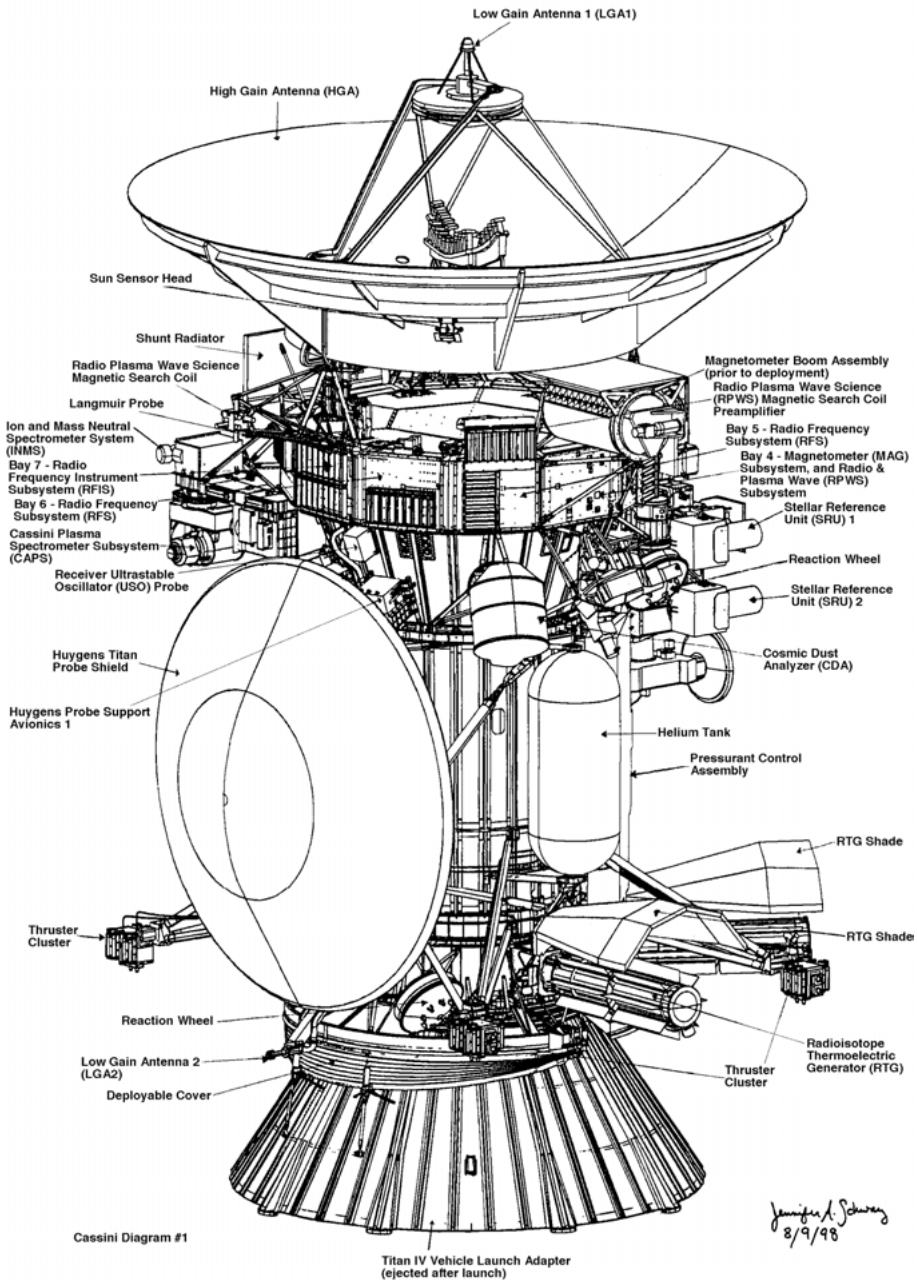


Figure 5.2. Artist's sketch of Cassini-Huygens with labelled instrumentation and components. Image credit: NASA Jet Propulsion Laboratory

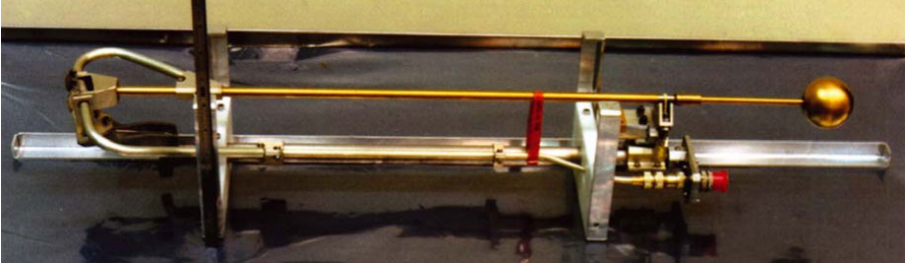


Figure 5.3. The Cassini RPWS Langmuir probe (LP) engineering model on its deployment boom in the folded configuration. Image reprinted from Gurnett et al. (2004) with permission from the publisher.

papers included in this thesis. In principle, a Langmuir probe measures the currents to and from the probe surface by collecting particles from the local plasma environment. Biasing the probe at positive or negative potentials attracts or repels electrons and ions, respectively. It was operated in two modes, sweeps and fixed-bias sampling. In the former, sweeping through bias voltages gives a current-voltage ( $I$ - $V$ ) curve. In the latter, the probe is kept at a fixed bias voltage, and the measured continuous current is converted to electron densities by calibration against the wave-derived densities from RPWS. Changes in spacecraft potential or electron temperature will change this linear scaling factor and thus need to be taken into account when sampling over longer periods. During the proximal orbits, the LP measurements alternated between sweeps and fixed-bias. Sweeps were conducted every 32 s (48 s for orbit 288), stepping through  $-4$  to  $+4$  V in 256 bias voltage steps (Morooka et al., 2019). The fixed-bias (3.74 V in the ionosphere) data was sampled at 20 Hz for orbits 283, 287, and 292, and at 1 Hz for orbit 288.

The measured current to/from the probe is generally split into three components: An electron current  $I_e$ , an ion current  $I_i$ , and secondary currents  $I_{se}$  caused by emission of electrons and ions from the probe surface. The latter are either due to the photoelectric effect from energetic photons (Einstein, 1905), referred to as the photoelectron current  $I_{ph}$ , or particle impact at high velocities. In a tenuous plasma, the photoelectron current generally is the dominant contribution to the secondary current. But in denser regions, such as those sampled during the proximal orbits, the secondary currents from particle impact at high velocities can quickly exceed  $I_{ph}$ . It should be noted that the spacecraft itself likewise collects these currents and, in equilibrium, its spacecraft potential will change so that the currents ultimately add up to zero.

$$I_{tot} = I_e + I_i + I_{se} = 0 \text{ (in equilibrium)} \quad (5.2)$$

How the different currents relate to other physical quantities such as temperatures, masses, and densities is dependent on a multitude of factors, such as the geometry of the probe, the energy distribution of the plasma, and the ratio be-

tween probe radius  $r_p$  and plasma Debye length  $\lambda_D$ , which determines whether orbital motion limited or sheath limited theory must be applied. For probe radii much smaller than the plasma Debye length, the former is applicable, whereas for ratios  $r_p/\lambda_D < 1$ , the latter should generally be used. With a few assumptions about the local plasma and knowledge of LP analysis techniques, the plasma characteristics can then be derived from the measured current. A sufficiently detailed description of these factors and theories to be of use to the reader exceeds the scope of this thesis. The intrigued reader may wish to consult, for example, Johansson et al. (2022) and Morooka et al. (2019) for details on the Cassini LP analysis and Darian et al. (2019), Laframboise and Parker (1973), and Mott-Smith and Langmuir (1926) for an overview of the fundamental theory.

As certain assumptions have to be made during the fitting of the sweeps, the analysis is not straightforward and may yield different interpretations and thus derived quantities. Some examples of LP analyses for the final orbits are shown in Morooka et al. (2019) and Johansson et al. (2022), which differ in their overall derived quantities as the latter attributes a much larger part of the current to neutral-impact induced secondary electron emission.

## 5.2 Ion and Neutral Mass Spectrometer (INMS)

Complementing the data from RPWS/LP, the Ion and Neutral Mass Spectrometer (INMS) provided unprecedented insights into the mass composition and number densities of neutral species and positive ions throughout the Cassini mission. It was a collaborative effort involving teams at NASA's Goddard Space Flight Center, the University of Michigan and Southwest Research Institute. Of particular focus during the development were the study of Titan's atmosphere, Saturn's magnetosphere and the ring environment. A comprehensive description of its design, calibration, and operation is provided by Waite et al. (2004). In the following description, the alphabetic labels in parentheses refer to the corresponding labelled components in Figure 5.4. The main components of INMS were its two sources (open and closed, a and b), a quadrupole lens for switching between those sources (c), electrostatic ion focusing lenses (d, also within a and b), a dual radio frequency quadrupole mass analyser (e) and two secondary electron multiplier detectors (f).

Operations were split between a closed source neutral mode to sample non-reactive neutral species (e.g.,  $H_2$ ,  $N_2$ ,  $CH_4$ , noble gases), an open source neutral beaming mode to measure reactive species (e.g. atomic nitrogen) and an open source ion mode, which sampled positive ions with energies below 100 eV (Waite et al., 2004). The open source (b) directly sampled the inflowing plasma and due to its narrow field of view of  $\sim 3^\circ$  was required to point close to the ram vector for optimal sensitivity. In contrast, the closed source (a) uses the ram pressure of the inflowing gas to produce a density enhance-

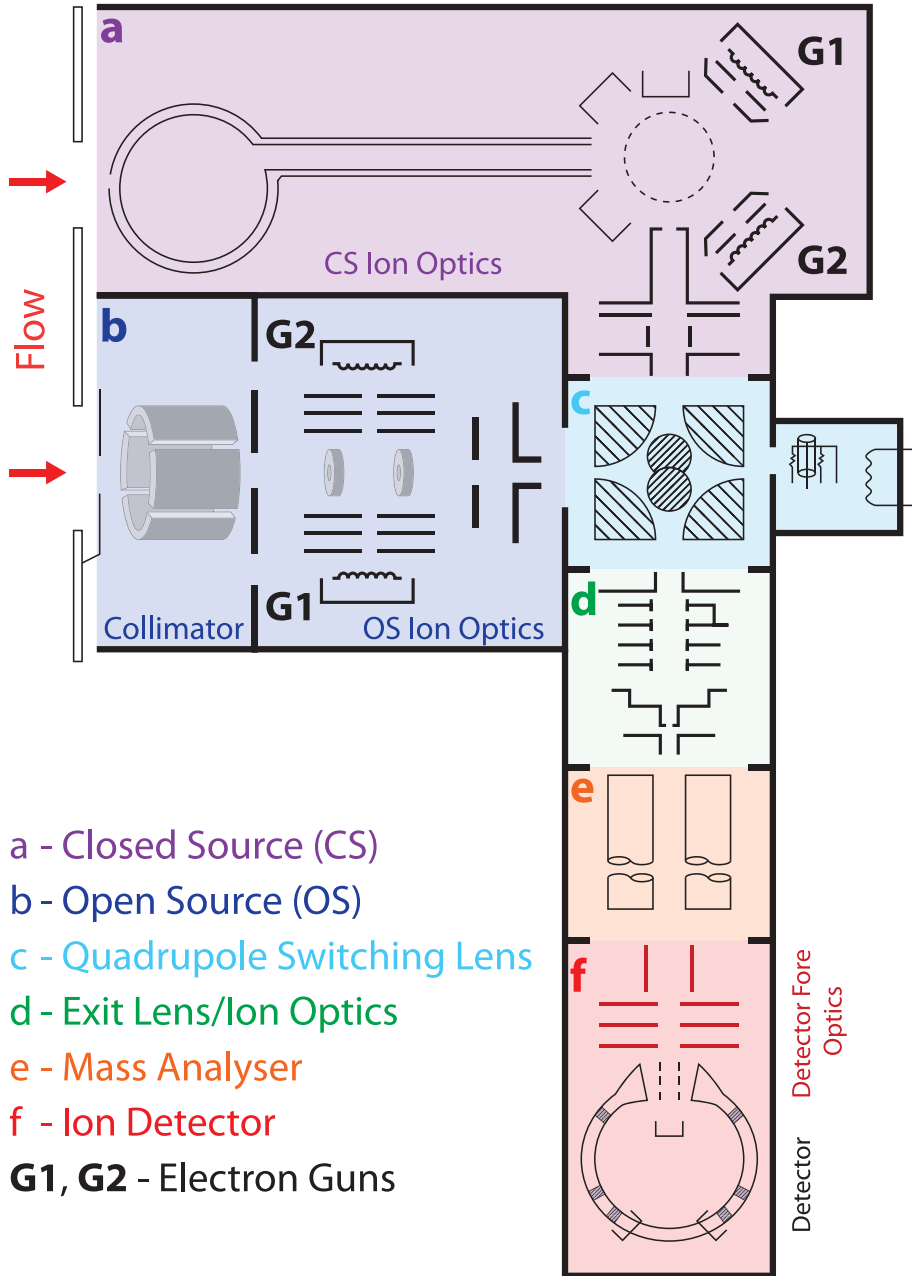


Figure 5.4. Schematic of the INMS depicting its two sources, the focusing and switching lenses, quadrupole mass analyser and the detector components. Image credit: Shebanits (2017), originally adapted from Mandt et al. (2012).

ment of the sampled species in the enclosed antechamber, which allowed for detection of neutrals with lower concentrations ( $\geq 10^4 \text{ cm}^{-3}$ , compared to  $\geq 10^5 \text{ cm}^{-3}$  for the open source). In the neutral modes, the electron guns (G1 and G2) ionized the sampled species before they passed through the quadrupole switching lens (c). During the proximal orbits analysed in this thesis, open source ion measurements were interspersed with closed source neutral mode measurements.

To sample any species at optimal sensitivity, the voltages of the quadrupole switching lens and the mass analyzer had to be adjusted to its particular mass and energy per charge. This required certain preassumptions during the proximal orbits on spacecraft charging and along-track ion flow velocities, as these alter the energy per charge ratio of incident particles. For each sampled species, the counts  $C_j$  were integrated for  $\Delta t = 31$  ms and converted to number densities  $n_j$  with the relation  $C_j = (10^{-5} n_j) / (S_j u_{s/c} \Delta t)$ , with the mass-dependent sensitivity factor  $S_j$  and spacecraft speed  $u_{s/c}$  in km/s (Cravens et al., 2019b). The instrument offered a detectable mass range of 1–99 Da and a mass resolution of 100 at 10% mass peak height (Waite et al., 2004). For the proximal orbits sampled during the Grand Finale, ion measurements were limited to species with mass-to-charge ratios  $< 8$  Da due to the high spacecraft speed of  $> 30$  km/s, which precluded direct detection of heavier ions due to their energies exceeding instrument capabilities. This is visible as discrepancies between ion and electron densities in regions where heavier ions become more abundant, such as the altitudes below  $\sim 2300$  km around closest approaches of orbits 288 and 292. The measurement of neutral species was complicated by the effects of chemistry within the antechamber, impact fragmentation of larger organic compounds and dust grains, and adsorption (certain species, such as  $\text{H}_2\text{O}$  and  $\text{NH}_3$ , exhibit a proclivity to stick to the antechamber walls). The derivation of densities for such species requires correction for the above effects and deconvolution of the mass spectra (for more detailed descriptions, see Miller et al., 2020; Serigano et al., 2022; Waite et al., 2018).

INMS data were used extensively for the analyses presented in the included papers. The open source ion measurements were only conducted for the proximal orbits 283, 287, 288, and 292, and since they are required for all presented methods, our analyses are limited to these orbits. The observable small-scale variations in  $\text{H}_2^+$  densities described in Paper III and the close match to the fixed-bias LP electron densities, once corrected for the timestamp shift as illustrated in Papers III and V, showcase the capabilities of both instruments. As CAPS was non-operational during the proximal orbits and thus unable to complement the INMS measurements, we have limited information on particle kinetics. While the ion energy can be constrained when varying the voltages of the quadrupole mass analyser for a given mass-to-charge ratio, as described in Cravens et al. (2019a), this required a special operational mode (energy scans were only conducted during orbit 287) and cannot fully replace the capabilities of a high-resolution energy spectrometer such as CAPS.

## 6. Summary of Publications

### 6.1 Paper I

*Constraining the Positive Ion Composition in Saturn's Lower Ionosphere with the Effective Recombination Coefficient*

**Dreyer, J.**, Vigren, E., Morooka, M., Wahlund, J.-E., Buchert S. C.,  
Johansson, F. L., and Waite, J. H. (2021)  
The Planetary Science Journal, 2.1, p. 39. doi:10.3847/psj/abd6e9

As the INMS ion measurements for the proximal orbits of the Grand Finale were limited to mass-to-charge ratios of  $< 8$  Da due to the high spacecraft speed of up to  $\sim 34$  km/s, the overall plasma composition of Saturn's equatorial ionosphere was not possible to measure directly. We present a method to estimate upper limits for the effective recombination coefficient at 300 K,  $\alpha_{300}$ , and thus constrain the positive ion composition in Saturn's equatorial ionosphere. The study focuses on data from two orbits, 288 and 292, for which all required measurements are available. As described in Section 4.2, the equatorial ionosphere is subject to an influx of ring material from the D ring. This not only affects the ionospheric plasma chemistry, but is also likely to result in some level of electron depletion due to attachment to dust grains. While we are not able to quantify the grain charging, a precise determination of the grain attachment and detachment rates is not necessary for our method of estimating upper limits of the effective recombination coefficient, as outlined in the paper. The resulting effective recombination coefficient is essentially a weighted average of the recombination coefficients of all present ion species, and can thus not exclude the presence of any species, but sufficiently constrain which ions are likely to be dominant.

We derive a median upper limit of  $\alpha_{300} = 1.93 \times 10^{-7} \text{ cm}^3 \text{ s}^{-1}$  across all orbits below 2000 km, which is lower than expected when comparing with model predictions for the dominant ion species. Water group and hydrocarbon ions, which have been previously suggested as abundant in this region, have recombination coefficients  $> 5 \times 10^{-7} \text{ cm}^3 \text{ s}^{-1}$  and are thus incompatible (at least as dominant species) with our derived upper limits. Suggestions for species with sufficiently low recombination coefficients include  $\text{HCNH}^+$  and  $\text{HCO}^+$ , of which the latter is a more likely candidate based on the model predictions by Moore et al. (2018) and *Case B* as modelled by Moses et al. (2023). It should be noted that this analysis was based on the LP-derived electron and ion densities, with the analysis by Morooka et al. (2019) indicating pronounced

levels of electron depletion around closest approaches. If we were instead to follow the results of Johansson et al. (2022) and utilize  $n_e = n_i$ , our derived upper limits would increase by approximately a factor of 3 and become more compatible with water group and hydrocarbon ions.

**My contribution:**

I participated in the conceptualization of the study and design of the methodology and had the main responsibility for the data analysis, project administration, and writing of the paper.

## 6.2 Paper II

*Empirical Photochemical Modeling of Saturn's Ionization Balance Including Grain Charging*

Vigren, E., **Dreyer, J.**, Eriksson, A., Johansson, F. L., Morooka, M., and Wahlund, J.-E. (2022)

The Planetary Science Journal, 3.2, p. 49. DOI:10.3847/psj/ac4eee

We develop a semi-analytical photochemical model of Saturn's equatorial ionosphere, building on the model by Cravens et al. (2019b) to include a more complex photochemistry and include the grain charging formalism from Draine and Sutin (1987). This allows us to further investigate the nature of M- and R-type species (which react with both  $H^+$  and  $H_3^+$  for the former and only with  $H_3^+$  for the latter) and the level of electron attachment to grains.

The model was applied to two regions of Cassini's orbit 292, 1700 and 2200 km above the 1 bar level. Particularly near 1700 km the model yields vastly different abundances of the two species types when compared to those derived from closed-source neutral INMS measurements: The predicted mixing ratios of M-type species are approximately one order of magnitude too small and those for R-type species one too large. This *mixing ratio conundrum* is in line with the difficulties faced by Moore et al. (2018) to reconcile their modelled  $H^+$  and  $H_3^+$  densities with those observed by INMS. Our model further yields minimum electron-to-ion ratios of  $\sim 50\%$ , notably higher than prior estimates based on LP data, and prompts us to question the applicability of the idea of conducting spherical dust grains: For a self-consistent solution, extremely small grains with radii of  $< 3 \text{ \AA}$  are required, leading us to conclude that dust particles are unlikely to be the main carrier of negative charge in this region of Saturn's ionosphere.

**My contribution:**

I participated in the conceptualization of the study, validation of the methodology and contributed during review and editing.

## 6.3 Paper III

### *Identifying Shadowing Signatures of C Ring Ringlets and Plateaus in Cassini Data from Saturn's Ionosphere*

**Dreyer, J.,** Vigren, E., Johansson, F. L., Shebanits, O., Morooka, M., Wahlund, J.-E., Perryman, R. S., and Waite, J. H. (2022)  
The Planetary Science Journal, 3.7, p. 168. doi:10.3847/psj/ac7790

We investigate the nature of observed narrow decreases (dips) in the ionospheric  $\text{H}_2^+$  densities for the outbound part of Cassini's orbits 288 and 292, which we briefly mentioned in Paper I and hypothesized to be the source of ring substructures. To test this hypothesis, we trace solar rays through Saturn's rings onto Cassini's orbit and calculate the individual shadows of substructures called ringlets and plateaus in Saturn's C ring, which are regions with increased optical depth. Initially, the computed shadows and observed dips did not align, with an average discrepancy of  $\sim 15$  km.

An extensive investigation of this misalignment revealed an error in the archived INMS timestamps, which gradually shifted since 2013 due to a no longer maintained in-house correction and increasingly diverged from the spacecraft clock. This resulted in timing offsets of up to  $\sim -4$  s at the end of the mission. A comparison of the ion densities with the fixed-bias, high-resolution LP electron densities revealed a peak correlation at an additional offset of  $-1$  s for all analysed orbits. Although this additional component is based on a comparison of the two instruments, and thus could theoretically contain an error of the LP timestamps, we choose to include it in our correction since errors in both archived data sets seem unlikely and including it improves the alignment of the dips with the calculated shadows. After correction of the timestamps, the shadows precisely align with the observed dips, confirming the initial hypothesis.

We then proceed by further estimating optical depths for the ringlets and plateaus by comparing the  $\text{H}_2^+$  densities within the respective shadowed regions to those from the inbound (and thus unshadowed) parts of the orbits. The derived estimates agree very well with values derived from stellar occultation measurements. Due to the short lifetime of  $\text{H}_2^+$  ions, the appearance (or lack thereof) of these dips can also provide insight into the applicability of photochemical equilibrium. If no clear and narrow dips are visible (which is the case for orbits 283 and 287), we can infer that the transport timescales are sufficiently short to dilute the ion signature over their respective chemical lifetime. Since these are  $\sim 50$  s for the closest approach altitudes of orbits 283 and 287, we can estimate a lower limit for the flow speed of 0.3 km/s, which is in line with prior estimates by Cravens et al. (2019a). The non-applicability of PCE around the closest approaches of orbits 283 and 287 likewise aligns with prior estimates.

### **My contribution:**

I had the main responsibility for the conceptualization of the study, methodology, data analysis, project administration, writing of the paper, and discovered the time shift in the INMS data (for which F.L.J. ultimately found the cause).

## 6.4 Paper IV

### *Utilizing Helium Ion Chemistry to Derive Mixing Ratios of Heavier Neutral Species in Saturn's Equatorial Ionosphere*

**Dreyer, J., Vigren, E., Johansson, F. L., and Waite, J. H. (2023)**

Journal of Geophysical Research: Space Physics, 128.6, e2023JA031488.

DOI:10.1029/2023ja031488

While a surprisingly large rate of ring influx from the D ring into Saturn's equatorial ionosphere has been established from the Grand Finale (e.g., Hsu et al., 2018; Mitchell et al., 2018; Waite et al., 2018), the mixing ratios of these heavier neutrals are difficult to measure directly due to the high spacecraft speed of  $\sim 34$  km/s complicating the analysis of the mass spectra. We devise a method to utilize helium ion chemistry to independently derive the mixing ratios of these heavier neutral species in Saturn's ionosphere.

Initially, we construct a simple photochemical model to show that the main loss process of helium ions at altitudes below 2500 km are not reactions with molecular hydrogen, but rather those with heavier neutral species, which we collectively refer to as X. We proceed by deriving an expression for the mixing ratio of these heavier species,  $f_X$ , based on the assumption of photochemical equilibrium and the measured densities for helium and hydrogen ions.

Our results show considerable inter- and intraorbital variability, which may suggest temporal or spatial changes in the ring influx. Overall, they fall below those derived from closed-source neutral INMS measurements as derived by Miller et al. (2020) and Serigano et al. (2022), which may indicate that only the most volatile ring-sourced species (CO, N<sub>2</sub> and CH<sub>4</sub>) significantly ablate to enter the gas phase in this region of Saturn's ionosphere and partake in the plasma chemistry, aligning with *Case B* as proposed by Moses et al. (2023).

### **My contribution:**

I had the main responsibility for the conceptualization of the study, methodology, data analysis, project administration, and writing of the paper.

## 6.5 Paper V

### *Electron to Light Ion Density Ratios During Cassini's Grand Finale: Addressing Open Questions About Saturn's Low-latitude Ionosphere*

**Dreyer, J., Vigren, E., Johansson, F. L., Hadid, L., Morooka, M.,  
Wahlund, J.-E., and Waite, J. H. (2023)**  
Manuscript in preparation

Finally, we try to address some remaining conundrums regarding the RPWS and INMS data from the Grand Finale. A comparison of the fixed-bias LP electron densities and the INMS light ion densities, enabled by the correction of the timestamp shift of the latter, shows strong positive correlation for most parts of the proximal orbits even on the short timescales of individual fixed-bias measurements, which we refer to as batches. Previously, the correlation was limited to larger timescales due to the timestamp misalignment. For this analysis, we study the variability in said correlation and the ratios of electron-to-light-ion densities, which we term scaling factors.

We detect three distinct regions for the analysed orbits 283, 287, 288 and 292 based on these two criteria: Region 1, which is found above altitudes of 2500 km and equatorward of  $\pm 20^\circ$  latitude, exhibits scaling factors less than 1 and overall strong positive correlation. This indicates a plasma mainly composed of light ions, as expected. While we explore several potential explanations for the low scaling factors, they essentially suggest that either the INMS light ion densities are overestimated or the measured electron densities are underestimated. Our ongoing analysis may also provide additional constraints on the electron temperature profile by comparing changes between LP fixed-bias, RPWS wave, and INMS ion data. Region 2 only occurs for orbits 288 and 292 below 2500 km, where the abundance of heavy ions is higher. This results in scaling factors above 1, and poor or even negative correlation between electron and light ion densities. Our analysis for Region 2 allows us to estimate lower limits for the number densities of heavier ion species, which are in line with recent modelling results by Moses et al. (2023). Lastly, Region 3 is located at latitudes poleward of approximately  $\pm 20^\circ$ , where the scaling factors rapidly rise far above 1 and correlation decreases. While further analysis of the conversion from raw instrument data to derived densities at these high altitudes is required, the rapid increase in scaling factors in both cases (based on LP fixed-bias or RPWS wave data) may indicate the presence of heavier ions, such as  $O^+$  and water group species, spiralling in from the C ring.

#### **My contribution:**

I had the main responsibility for the conceptualization of the study, methodology, data analysis, project administration, and writing of the paper.

## 7. Outlook

The proximal orbits of Cassini's Grand Finale gave us a much closer look at Saturn's equatorial ionosphere than ever before. But our fleeting view of this additional level of complexity brings about awareness of all the things we do not fully understand; for every insight the Grand Finale revealed, one more question was added to the to-do list.

Some of these questions include:

- At which altitudes do which species ablate and enter the gas phase to partake in the atmospheric chemistry, and are most grain-bound species likely to do this in the ionosphere or only the most volatile, as discussed by Moses et al. (2023) and in Paper IV? Why do models struggle so much to match the observed  $H^+$  and  $H_3^+$  densities? There seems to be something about the hydrogen chemistry in this region that we do not fully understand – is it purely the ratio of the proposed M- and R-type neutral species, as discussed by Cravens et al. (2019b) and in Papers II and IV, or are we missing some other process?
- How does the ionospheric circulation of this ring material look like? Is it most likely to be horizontally distributed at ionospheric altitudes or further down? How does the current system around the equator affect it (e.g. Khurana et al., 2018)?
- Why does the influx from the D ring seem to vary so much, both with latitude during an orbit and between successive orbits? Is it indeed a recent development, as suggested by Moses et al. (2023)? If not, how is this influx sustained over astronomical timescales, bearing in mind the rather miniscule mass of the D ring? Is it indeed supplied by inward transport from the C ring, as suggested by Waite et al. (2018)?

To address these open questions more concretely, future studies can explore various avenues. Zhang et al. (2023) model the effects of spacecraft charging in Saturn's ionosphere during the proximal orbits. By comparing with the prior work by Zhang et al. (2021) and LP analyses by Morooka et al. (2019) and Johansson et al. (2022), they find that secondary electron and ion emission can not easily be distinguished from the presence of negatively charged dust providing an environment where the positively charged plasma species are more mobile than the negative charge carriers. It is difficult to fully resolve this ambiguity without improving our understanding of the impact yields of the most important species. For example, no such measurements are available for titanium nitrate, with which the Cassini LP was coated. In addition, these yields are expected to change for a space-weathered probe, such as the Cassini LP at

the end of mission (Johansson et al., 2022). As a result, we resort to estimating these yields based on measurements of other materials, introducing an inherent uncertainty that is challenging to quantify. Future laboratory measurements of these yields may serve to retroactively improve the analyses for the Cassini LP, while also enabling similar analyses for future missions.

The behaviour of infalling ring material in the plasma of the ionosphere itself is an area with many gaps in our collective understanding. Once again, future laboratory measurements and insights gained from studying dusty plasmas in Earth's ionosphere may serve to improve our knowledge of, for example, grain charging theory, the ablation profile of these tiny particles, and their fragmentation patterns. Beyond this, further improvements of the models of Saturn's ionosphere and its interaction with the rings and magnetosphere will likely result from including grain charging, incorporating the electrodynamics revealed during the Grand Finale, and expanding to three-dimensional models. All of this will be of much benefit to improve the comparison between model output, such as that of Moses et al. (2023), and the in situ data. Additional experimental and theoretical constraints on the rates of certain reactions, such as the loss of  $H^+$  with vibrationally excited hydrogen and sources thereof (e.g., Chang et al., 2021; Huestis, 2008), may also improve these models.

Considering the exceedingly unlikely prospect of another up-close visit to Saturn's equatorial ionosphere in the foreseeable future, our understanding will continue to rely on advances in atmospheric models and remote observations. The capabilities of ground- and space-based telescopes have advanced significantly in recent years, and it seems likely that they will fill the hole that Cassini's demise left behind. Observations with telescopes surveying a range of wavelengths are revealing a host of new discoveries, such as the measurements of absolute wind speeds with the Atacama Large Millimeter/Submillimeter Array (ALMA) by Benmahi et al. (2022) or the additional constraints on the abundance of atomic hydrogen ions based on a comparison of Hubble observations with Cassini data by Ben-Jaffel et al. (2023). It may not be so far-fetched for future remote measurements to constrain the abundances of certain species, for example  $HCO^+$ , and extend our ephemeral data from the Grand Finale to longer timescales. This could also allow us to answer questions regarding the potentially transient nature and evolution of the influx from the D ring. Likewise, future missions to the other outer planets, such as the recently launched Jupiter Icy Moons Explorer (JUICE), may provide additional indirect insights via comparative planetology.

I sincerely hope that the research presented in this thesis proves valuable to those studying this remarkable planet in the future and I have added some load-bearing grains of sand to the monumental sandcastle that is our collective understanding of the universe.

## 8. Sammanfattning på svenska

Gasjätten Saturnus, den näst största av planeterna i solsystemet, har länge varit en källa till undran och inspiration. Mänsklighetens tidigare besök, med Pioneer- och Voyager-rymdfarkosterna, var flyktiga möten på relativt stora avstånd från planeten. Rymdfarkosten Cassini-Huygens, som sköts upp 1997, anlände till Saturnussystemet 2004 och tillbringade många år med att undersöka jätten, dess månar och berömda ringar på nära håll. Mellan april och september 2017 avslutade Cassini sina nära 13 år kring Saturnus med en serie djärva dykningar mellan ringarna och de övre delarna av Saturnus atmosfär. Denna sista fas av uppdraget, kallad *Grand Finale*, avslöjade en mycket varierande jonosfär under påverkan av ett förvånansvärt stort inflöde av ringmaterial från Saturnus innersta D-ring. De artiklar som ingår i denna avhandling presenterar några insikter nådda utifrån analys av data som samlats in under dessa nära omloppsbanor.

Inledningsvis härleder vi övre gränser för den effektiva rekombinationskoefficienten i Saturnus ekvatoriella jonosfär på höjder under 2500 km, där fotokemisk jämvikt kan antas, för att få ledtrådar till sammansättningen av den tyngre joner. Våra resultat indikerar vid första anblick en rik förekomst av joner karakteriserade av låg rekombinationskoefficient, såsom  $\text{HCO}^+$ , medan vatten- och komplexa kolvätejoner sannolikt inte är dominerande.

Vi följer upp detta genom att utveckla en semi-analytisk fotokemisk modell, som inkluderar laddning av rymddamm, för att undersöka effekterna av ringinflödet på plasmasammansättningen. Användning av modellen över regioner av Cassinis omloppsbana 292 ger mycket olika förekomster av två familjer av molekyler jämfört med de uppmätta av masspektrometern INMS, i synnerhet kring 1700 km över 1 bar-nivån. Detta kan direktkopplas till svårigheten att förena de observerade  $\text{H}^+$ - och  $\text{H}_3^+$ -densiteterna med våra och andras modellresultat. Vi beräknar också ett lägsta elektron-till-jon-täthetsförhållande på  $\sim 50\%$ , vilket överstiger tidigare uppskattningar baserade på mätningar från farkostens Langmuirsond (LP). För en heltäckande lösning krävs extremt små dammkorn med radier på  $< 3 \text{ \AA}$  vilket leder till att vi drar slutsatsen att dammpartiklar sannolikt inte är den huvudsakliga bäraren av negativ laddning i denna region av Saturnus jonosfär.

Nästa steg är att karakterisera observerade minskningar (smala nedgångar) i de jonosfäriska  $\text{H}_2^+$  densiteterna. För detta ändamål spårar vi solstrålar genom Saturnus ringar till Cassinis omloppsbana och förutsäger de individuella skuggorna från understrukturer i Saturnus C-ring, vilka är områden med ökad optiskt djup. Inledningsvis stämde de beräknade skuggorna och de observerade fallen i  $\text{H}_2^+$ -täthet inte överens, med en genomsnittlig avvikelse på

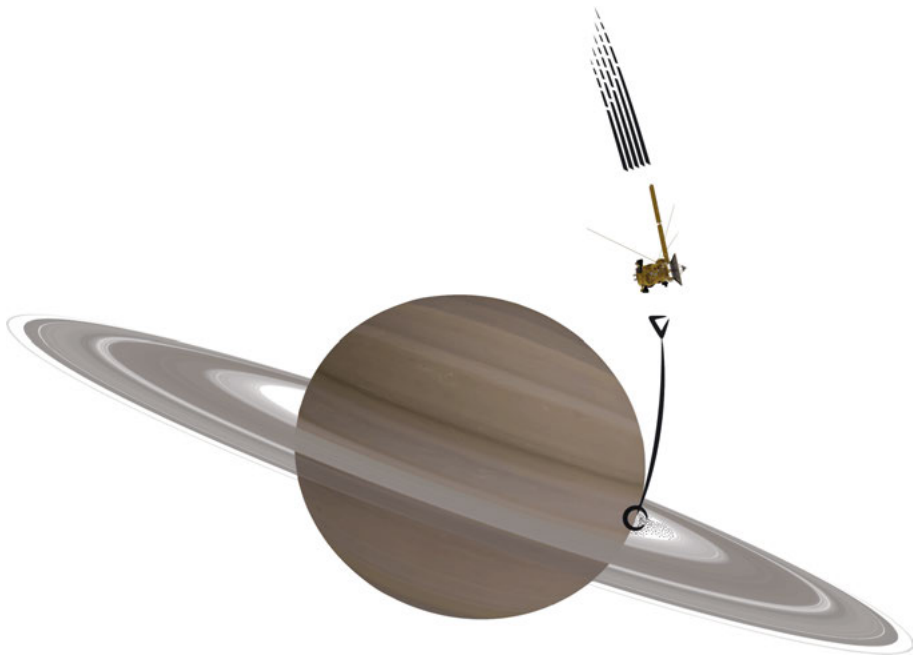
cirka 15 km. En omfattande undersökning av detta fel i överensstämmelse avslöjade ett fel i de arkiverade INMS-tidsstämplarna, som gradvis förändrats sedan 2013 på grund av en intern korrigerings som inte längre fanns kvar. Detta resulterade i allt högre avvikelser från rymdfarkostens klocka och i tidsförskjutningar på upp till  $-4$  s vid uppdragets slut. En jämförelse av jondensiteterna med de högupplösta LP-elektronensiteterna visade en optimal korrelation vid en ytterligare förskjutning på  $-1$  s för alla analyserade banor. Efter korrigerings av tidsstämplarna stämmer de förutsagda skuggorna exakt överens med de observerade minskningarna i koncentrationen av  $H_2^+$ . Vi fortsätter med att ytterligare uppskatta ringstrukturernas optiska djup genom att jämföra  $H_2^+$ -densiteterna inom skuggade områden med de i solljus. De härledda uppskattningarna överensstämmer mycket väl med värden som framtagits från mätningar av stjärnokkultationer. På grund av den korta livslängden för  $H_2^+$ -joner kan uppträdet (eller bristen därav) av dessa nedgångar också utvärdera tillämpligheten av antagandet om fotokemisk jämvikt. Om inga tydliga och smala nedgångar är synliga (vilket är fallet för omloppsbanorna 283 och 287) kan vi dra slutsatsen att transporttidsskalorna är tillräckligt korta för att späda ut jonsignaturen under deras kemiska livslängd. Eftersom dessa är cirka 50 s för de närmaste inflygningshöjderna på omloppsbanorna 283 och 287 kan vi uppskatta en nedre gräns för flödes hastigheten på 0.3 km/s, vilket är i linje med tidigare uppskattningar.

Från Grand Finale har en förvånansvärt kraftig tillströmning av ringmaterial från D-ringen till Saturnus ekvatoriella jonofär etablerats. Blandningsförhållandena av dessa tyngre neutrala ämnen är dock svåra att mäta direkt på grund av rymdfarkostens höga hastighet på upp till  $\sim 34$  km/s, vilket komplicerar analysen av masspektra. Vi tar fram en metod för att använda heliumjonkemi för att oberoende härleda blandningsförhållandena för dessa tyngre neutrala ämnen i Saturnus jonofär. Inledningsvis konstruerar vi en enkel fotokemisk modell för att visa att den främsta förlustprocessen för heliumjoner på höjder under 2500 km inte är reaktioner med molekylärt väte, utan snarare de med tyngre neutrala ämnen. Vi fortsätter med att härleda ett uttryck för blandningsförhållandet för dessa tyngre ämnen baserat på antagandet om fotokemisk jämvikt och de uppmätta densiteterna för helium- och vätejoner. Våra resultat visar på betydande variationer inom enskilda banor och banor emellan, vilket kan antyda temporala eller rumsliga förändringar i inflöde av ringmaterial. Totalt sett ligger blandningsförhållandena under de som härleds från INMS-mätningar, vilket kan indikera att endast de mest flyktiga ämnena ( $CO$ ,  $N_2$  och  $CH_4$ ) i betydande grad evaporerar från infallande ringpartiklar (och därmed påverkar plasmakemin) i den här regionen av Saturnus jonofär.

Slutligen försöker vi ta itu med några återstående gåtor angående elektron- och jondata från Grand Finale. En jämförelse av de högupplösta LP-elektronensiteterna och INMS-lättjontätheterna (upp till  $He^+$ ), möjliggjord genom den ovan nämnda korrigerings av INMS tidsstämpel, visar en stark positiv korrelation för merparten av de närliggande omloppsbanorna, även på

korta tidsintervall. För denna analys studerar vi variationen i denna korrelation och förhållandena mellan elektron- och lättjondensiteter, som vi kallar skalningsfaktorer. Vi upptäcker tre tydliga regioner för de analyserade omloppsbanorna 283, 287, 288 och 292 baserat på dessa två kriterier: Region 1, som återfinns ovanför höjder på 2500 km och mellan  $+20^\circ$  och  $-20^\circ$  latitud, uppvisar skalningsfaktorer  $< 1$  och överlag stark positiv korrelation, vilket indikerar ett plasma bestående av lätta joner, som förväntat. Orsaken till de låga skalningsfaktorerna är under utredning och pågående analys kan även ge ytterligare begränsningar för elektronens temperaturprofil. Region 2 syns endast för omloppsbanorna 288 och 292 under 2500 km, där förekomsten av tunga joner är högre. Detta resulterar i skalningsfaktorer  $> 1$ , och dålig eller till och med negativ korrelation mellan elektron- och lättjondensiteter. Slutligen är Region 3 belägen på latituder norr eller söder om cirka  $\pm 20^\circ$ , där skalningsfaktorerna snabbt stiger långt över 1 och korrelationen minskar. Detta kan indikera närvaron av tyngre joner (exempelvis  $O^+$  eller vattengruppjoner) som spiraliserar in längs magnetfältslinjerna från C-ringen.

Även om många öppna frågor kvarstår, såsom sammansättningen av ringinflödet och var det främst ablaterar i den övre atmosfären, hur variabelt det är och om det är ett nyligen inträffat fenomen, så kastar resultaten som presenteras i denna avhandling ytterligare ljus över Saturnus ekvatoriella jonosfär.



*Figur 8.1.* Illustration av Cassini-rymdfarkosten på väg mot tillintetgörelse i Saturnus övre atmosfär. Figur anpassad från modellavbildningar av Saturnus och Cassini tillhandahållna av NASA.

# Acknowledgements

First and foremost, I want to thank Erik for being the best supervisor anyone could ask for, his infallible ability and willingness to endure and interpret my incoherent stream of consciousness, and making the past few years so enjoyable! I had a ton of fun bouncing ideas off each other, discussing science, politics, and the general state of the world and look forward to more of the same whenever the opportunity presents itself. I would also like to thank my co-supervisors, Michiko and Jan-Erik, for always being available for questions and their encouragement and support along the journey. The same goes for Hunter, and for his ability and patience in explaining the inner workings of INMS to me. My gratitude to all the others who have provided guidance and mentorship in the past years, among them Anders, Noora, and Yuri.

I felt very at home in Uppsala and at IRF these past years, which I attribute to the great people I had the pleasure of interacting with on a daily basis. Thanks to all my fellow PhDs and postdocs for the good times; I wish I had already got to know you better during the first two years of my time here. I couldn't have asked for a nicer office mate to welcome and teach me the dark ways of science than Fredrik, wise beyond his years, and his follow-up, Jordi, who took over this role with much grace and endured me constantly letting the frigid polar air inside. The Svalbard 2022 gang: Ahmad, Henriette, Ida (special thanks for checking Chapter 8), Jordi, Louis, and the rest of the international bunch - thanks for making the return into darkness so enjoyable, you had some big shoes to fill! And the others whose company I got to enjoy and learn from these past years: Andreas, Elias, Elisabeth, Katerina, Konrad, Konstantin, Oleg, the astronomers and the KTHers, and so many more<sup>1</sup> – I hope you enjoy(ed) it here as much as I did.

While the first two years or so weren't exactly blissful due to the pandemic, a huge thanks goes to all my friends (local, international, everywhere) and colleagues for making those times as enjoyable and productive as they were and for keeping me reasonably sane<sup>2</sup> in the process. A special thanks to the Rats, *Die Gruppe*, and the D&D gang for the countless hours of fun company and enduring all my northern German humour, which undoubtedly lives up to the dreaded stereotypes. And, not to be forgotten, a massive thank you and much love to my family for their unwavering support throughout the years and for dealing with my idiosyncrasies.

---

<sup>1</sup>I can't possibly name all the "senior" scientists without this becoming even more excessive.

<sup>2</sup>This is a point of much contention.

I would also like to thank the citizens of Sweden and Norway for so readily and warmly welcoming me in both countries and to the EU for making my studies abroad possible and highly enjoyable.

Many illustrations in this thesis were created by NASA/JPL, and the cover art is my adaptation of the Saturn and Cassini models provided by NASA Visualization Technology Applications and Development, using Inkscape and Affinity Designer. My sincere thanks to all the artists, designers, and programmers behind these incredible works.

The fact that as a species, we can sample minuscule variations in the densities of electrons and ions around another planet over a billion kilometres away from our own, while precisely steering the instrument of such collective ingenuity through said planet's upper atmosphere, will never cease to amaze me. The fact that this was accomplished with technology as ancient as me only adds to this amazement. A very genuine thank you to all those who made this thesis possible with their hard work over Cassini's nearly three-decade journey – from its conception in a scratchbook, undoubtedly alongside many mugs of coffee, to the crafting of the incredibly complex array of intertwined instrumentation, and ultimately, the operation and analysis conducted during its twenty years in space and since its demise above the clouds of Saturn.

This has been an enlightening and fun journey for me, which likely began way back with an initial fascination for space but became more direct with Cassini's final moments – an event that an international master's student from Germany witnessed back on 15 September 2017 in a lecture hall at BMC in Uppsala<sup>1</sup>. I certainly would not have guessed as much at the time, but in some roundabout way, it seems very fitting that I ended up working with the very data from said *Grand Finale* and some of the people in that lecture hall.

And finally, the last thanks go to you, the reader, for staying committed until the end!<sup>2</sup>



Figure 9.1. The funeral of Cassini, rest in peace.

<sup>1</sup>Before attending a gasque later that day, which feels appropriately festive in retrospect.

<sup>2</sup>You didn't skip here, did you?

# References

- Atreya, S. K. and T. M. Donahue (1975). “Ionospheric models of Saturn, Uranus, and Neptune”. In: *Icarus* 24.3, pp. 358–362. doi: 10.1016/0019-1035(75)90131-1.
- Baines, K. H. et al., eds. (2018). *Saturn in the 21st Century*. Cambridge University Press. doi: 10.1017/9781316227220.
- Barrow, D. J. and K. I. Matcheva (2013). “Modeling the effect of atmospheric gravity waves on Saturn’s ionosphere”. In: *Icarus* 224.1, pp. 32–42. doi: 10.1016/j.icarus.2013.01.027.
- Baumjohann, W. and R. A. Treumann (1996). *Basic Space Plasma Physics*. Published By Imperial College Press and Distributed By World Scientific Publishing Co. doi: 10.1142/p015.
- Ben-Jaffel, L. et al. (2023). “The Enigmatic Abundance of Atomic Hydrogen in Saturn’s Upper Atmosphere”. In: *The Planetary Science Journal* 4.3, p. 54. doi: 10.3847/psj/acaf78.
- Benmahi, B. et al. (2022). “First absolute wind measurements in Saturn’s stratosphere from ALMA observations”. In: *Astronomy & Astrophysics* 666, A117. doi: 10.1051/0004-6361/202244200.
- Brown, Z. et al. (2020). “A pole-to-pole pressure–temperature map of Saturn’s thermosphere from Cassini Grand Finale data”. In: *Nature Astronomy* 4.9, pp. 872–879. doi: 10.1038/s41550-020-1060-0.
- Burton, M. E., M. K. Dougherty, and C. T. Russell (2010). “Saturn’s internal planetary magnetic field”. In: *Geophysical Research Letters* 37.24. doi: 10.1029/2010gl1045148.
- Capone, L. A. et al. (1977). “The ionospheres of Saturn, Uranus, and Neptune.” In: *Astrophysical Journal* 215, pp. 977–983. doi: 10.1086/155434.
- Chadney, J. M. et al. (2022). “Energy deposition in Saturn’s equatorial upper atmosphere”. In: *Icarus* 372, p. 114724. doi: 10.1016/j.icarus.2021.114724.
- Chang, Y. et al. (2021). “Vibrationally excited molecular hydrogen production from the water photochemistry”. In: *Nature Communications* 12.1, p. 6303. doi: 10.1038/s41467-021-26599-9.
- Coates, A. J. et al. (2007). “Discovery of heavy negative ions in Titan’s ionosphere”. In: *Geophysical Research Letters* 34.22, p. L22103. doi: 10.1029/2007gl1030978.
- Coates, A. et al. (2010). “Negative ions in the Enceladus plume”. In: *Icarus* 206.2, pp. 618–622. doi: 10.1016/j.icarus.2009.07.013.

- Colwell, J. E., L. W. Esposito, and J. H. Cooney (2018). “Particle sizes in Saturn’s rings from UVIS stellar occultations 1. Variations with ring region”. In: *Icarus* 300, pp. 150–166. doi: 10.1016/j.icarus.2017.08.036.
- Colwell, J. E. et al. (2009). “The structure of Saturn’s rings”. In: *Saturn from Cassini-Huygens*. Ed. by M. K. Dougherty, L. W. Esposito, and S. M. Krimigis. Springer Netherlands, pp. 375–412. doi: 10.1007/978-1-4020-9217-6\_13.
- Connerney, J. E. P. (1986). “Magnetic connection for Saturn’s rings and atmosphere”. In: *Geophysical Research Letters* 13.8, pp. 773–776. doi: 10.1029/GL013i008p00773.
- Connerney, J. E. P. and J. H. Waite (1984). “New model of Saturn’s ionosphere with an influx of water from the rings”. In: *Nature* 312.5990, pp. 136–138. doi: 10.1038/312136a0.
- Cravens, T. E. et al. (2019a). “Plasma Transport in Saturn’s Low-Latitude Ionosphere: Cassini Data”. In: *Journal of Geophysical Research: Space Physics* 124.6. doi: 10.1029/2018ja026344.
- Cravens, T. E. et al. (2019b). “The Ion Composition of Saturn’s Equatorial Ionosphere as Observed by Cassini”. In: *Geophysical Research Letters* 46.12, pp. 6315–6321. doi: 10.1029/2018gl1077868.
- Cravens, T. E. (1997). *Physics of Solar System Plasmas*. Cambridge Atmospheric and Space Science Series. Cambridge University Press. doi: 10.1017/cbo9780511529467.
- Cuzzi, J. N., G. Filacchione, and E. A. Marouf (2018). “The Rings of Saturn”. In: *Planetary Ring Systems: Properties, Structure, and Evolution*. Ed. by M. S. Tiscareno and C. D. E. Murray. Cambridge Planetary Science. Cambridge University Press, pp. 51–92. doi: 10.1017/9781316286791.003.
- Cuzzi, J. et al. (2009). “Ring Particle Composition and Size Distribution”. In: *Saturn from Cassini-Huygens*. Ed. by M. K. Dougherty, L. W. Esposito, and S. M. Krimigis. Springer Netherlands, pp. 459–509. doi: 10.1007/978-1-4020-9217-6\_15.
- Darian, D. et al. (2019). “Theory and simulations of spherical and cylindrical Langmuir probes in non-Maxwellian plasmas”. In: *Plasma Physics and Controlled Fusion* 61.8, p. 085025. doi: 10.1088/1361-6587/ab27ff.
- Dougherty, M. K. et al. (2004). “The Cassini Magnetic Field Investigation”. In: *Space Science Reviews* 114.1-4, pp. 331–383. doi: 10.1007/s11214-004-1432-2.
- Dougherty, M. K., L. W. Esposito, and S. M. Krimigis, eds. (2009). *Saturn from Cassini-Huygens*. Springer Netherlands. doi: 10.1007/978-1-4020-9217-6.
- Draine, B. T. and B. Sutin (1987). “Collisional Charging of Interstellar Grains”. In: *The Astrophysical Journal* 320, pp. 803–817. doi: 10.1086/165596.
- Dreyer, J. et al. (2021a). “Characteristics of fragmented aurora-like emissions (FAEs) observed on Svalbard”. In: *Annales Geophysicae* 39.2, pp. 277–288. doi: 10.5194/angeo-39-277-2021.

- Dreyer, J. (2021). *Saturn's dusty equatorial ionosphere from Cassini's Grand Finale observations*. Licentiate thesis. Uppsala University, Department of Physics and Astronomy; Swedish Institute of Space Physics, Uppsala Division.
- Dreyer, J. et al. (2021b). "Constraining the Positive Ion Composition in Saturn's Lower Ionosphere with the Effective Recombination Coefficient". In: *The Planetary Science Journal* 2.1, p. 39. doi: 10.3847/psj/abd6e9.
- Dreyer, J. et al. (2022). "Identifying Shadowing Signatures of C Ring Ringlets and Plateaus in Cassini Data from Saturn's Ionosphere". In: *The Planetary Science Journal* 3.7, p. 168. doi: 10.3847/psj/ac7790.
- Dreyer, J. et al. (2023). "Utilizing Helium Ion Chemistry to Derive Mixing Ratios of Heavier Neutral Species in Saturn's Equatorial Ionosphere". In: *Journal of Geophysical Research: Space Physics* 128.6, e2023JA031488. doi: 10.1029/2023ja031488.
- Durisen, R. H. and P. R. Estrada (2023). "Large mass inflow rates in Saturn's rings due to ballistic transport and mass loading". In: *Icarus* 400, p. 115221. doi: 10.1016/j.icarus.2022.115221.
- Einstein, A. (1905). "Über einen die Erzeugung und Verwandlung des Lichtes betreffenden heuristischen Gesichtspunkt". In: *Annalen der Physik* 322.6, pp. 132–148. doi: 10.1002/andp.19053220607.
- Estrada, P. R. and R. H. Durisen (2023). "Constraints on the initial mass, age and lifetime of Saturn's rings from viscous evolutions that include pollution and transport due to micrometeoroid bombardment". In: *Icarus* 400, p. 115296. doi: 10.1016/j.icarus.2022.115296.
- Estrada, P. R. et al. (2015). "Combined structural and compositional evolution of planetary rings due to micrometeoroid impacts and ballistic transport". In: *Icarus* 252, pp. 415–439. doi: 10.1016/j.icarus.2015.02.005.
- Galand, M. et al. (2009). "Solar primary and secondary ionization at Saturn". In: *Journal of Geophysical Research: Space Physics* 114.6, pp. 1–17. doi: 10.1029/2008ja013981.
- Galand, M. et al. (2011). "Response of Saturn's auroral ionosphere to electron precipitation: Electron density, electron temperature, and electrical conductivity". In: *Journal of Geophysical Research: Space Physics* 116.A9. doi: 10.1029/2010ja016412.
- Galanti, E. et al. (2019). "Saturn's Deep Atmospheric Flows Revealed by the Cassini Grand Finale Gravity Measurements". In: *Geophysical Research Letters* 46.2, pp. 616–624. doi: 10.1029/2018gl1078087.
- Gurnett, D. A. et al. (2004). "The Cassini Radio and Plasma Wave Investigation". In: *Space Science Reviews* 114.1-4, pp. 395–463. doi: 10.1007/s11214-004-1434-0.
- Gurnett, D. A. et al. (2005). "Radio and Plasma Wave Observations at Saturn from Cassini's Approach and First Orbit". In: *Science* 307.5713, pp. 1255–1259. doi: 10.1126/science.1105356.

- Hadid, L. Z. et al. (2018). “Ring Shadowing Effects on Saturn’s Ionosphere: Implications for Ring Opacity and Plasma Transport”. In: *Geophysical Research Letters* 45.19, pp. 10084–10092. doi: 10.1029/2018gl1079150.
- Hadid, L. Z. et al. (2019). “Saturn’s Ionosphere: Electron Density Altitude Profiles and D-Ring Interaction From The Cassini Grand Finale”. In: *Geophysical Research Letters* 46.16, pp. 9362–9369. doi: 10.1029/2018gl1078004.
- Hamil, O. et al. (2018). “Fate of Ice Grains in Saturn’s Ionosphere”. In: *Journal of Geophysical Research: Space Physics* 123.2, pp. 1429–1440. doi: 10.1002/2017ja024616.
- Heays, A. N., A. D. Bosman, and E. F. v. Dishoeck (2017). “Photodissociation and photoionisation of atoms and molecules of astrophysical interest”. In: *Astronomy & Astrophysics* 602, A105. doi: 10.1051/0004-6361/201628742.
- Hedman, M. M. et al. (2009). “Organizing some very tenuous things: Resonant structures in Saturn’s faint rings”. In: *Icarus* 202.1, pp. 260–279. doi: 10.1016/j.icarus.2009.02.016.
- Hedman, M. M. et al. (2007). “Saturn’s dynamic D ring”. In: *Icarus* 188.1, pp. 89–107. doi: 10.1016/j.icarus.2006.11.017.
- Horányi, M. et al. (2009). “Diffuse Rings”. In: *Saturn from Cassini-Huygens*. Ed. by M. K. Dougherty, L. W. Esposito, and S. M. Krimigis. Springer Netherlands, pp. 511–536. doi: 10.1007/978-1-4020-9217-6\_16.
- Hsu, H. W. et al. (2018). “In situ collection of dust grains falling from Saturn’s rings into its atmosphere”. In: *Science* 362.6410. doi: 10.1126/science.aat3185.
- Huebner, W. F. and J. Mukherjee (2015). “Photoionization and photodissociation rates in solar and blackbody radiation fields”. In: *Planetary and Space Science* 106, pp. 11–45. doi: 10.1016/j.pss.2014.11.022.
- Huestis, D. L. (2008). “Hydrogen collisions in planetary atmospheres, ionospheres, and magnetospheres”. In: *Planetary and Space Science. Advances in Planetary Sciences: AOGS 2007* 56.13, pp. 1733–1743. doi: 10.1016/j.pss.2008.07.012.
- Iess, L. et al. (2019). “Measurement and implications of Saturn’s gravity field and ring mass”. In: *Science* 364.6445. doi: 10.1126/science.aat2965.
- Jerousek, R. G. et al. (2020). “Saturn’s C ring and Cassini division: Particle sizes from Cassini UVIS, VIMS, and RSS occultations”. In: *Icarus* 344. July 2019, p. 113565. doi: 10.1016/j.icarus.2019.113565.
- Johansson, F. L. et al. (2022). “Implications from secondary emission from neutral impact on Cassini plasma and dust measurements”. In: *Monthly Notices of the Royal Astronomical Society* 515.2, pp. 2340–2350. doi: 10.1093/mnras/stac1856.
- Kempf, S. et al. (2023). “Micrometeoroid infall onto Saturn’s rings constrains their age to no more than a few hundred million years”. In: *Science Advances* 9.19, eadf8537. doi: 10.1126/sciadv.adf8537.

- Khurana, K. K. et al. (2018). “Discovery of Atmospheric-Wind-Driven Electric Currents in Saturn’s Magnetosphere in the Gap Between Saturn and its Rings”. In: *Geophysical Research Letters* 45.19. doi: 10.1029/2018g1078256.
- Kim, Y. H. et al. (2014). “Hydrocarbon ions in the lower ionosphere of Saturn”. In: *Journal of Geophysical Research: Space Physics* 119.1, pp. 384–395. doi: 10.1002/2013ja019022.
- Kliore, A. J. et al. (2009). “Midlatitude and high-latitude electron density profiles in the ionosphere of Saturn obtained by Cassini radio occultation observations”. In: *Journal of Geophysical Research: Space Physics* 114.A4. doi: 10.1029/2008ja013900.
- Kollmann, P. et al. (2018). “Saturn’s Innermost Radiation Belt Throughout and Inward of the D-Ring”. In: *Geophysical Research Letters* 45.20, pp. 10, 912–10, 920. doi: 10.1029/2018g1077954.
- Krimigis, S. M. et al. (2004). “Magnetosphere Imaging Instrument (MIMI) on the Cassini Mission to Saturn/Titan”. In: *Space science reviews* 114.1-4, pp. 233–329. doi: 10.1007/s11214-004-1410-8.
- Krimigis, S. M. et al. (2005). “Dynamics of Saturn’s Magnetosphere from MIMI During Cassini’s Orbital Insertion”. In: *Science* 307.5713, pp. 1270–1273. doi: 10.1126/science.1105978.
- Laframboise, J. G. and L. W. Parker (1973). “Probe design for orbit-limited current collection”. In: *The Physics of Fluids* 16.5, pp. 629–636. doi: 10.1063/1.1694398.
- Majeed, T. and J. C. McConnell (1991). “The upper ionospheres of Jupiter and Saturn”. In: *Planetary and Space Science* 39.12, pp. 1715–1732. doi: 10.1016/0032-0633(91)90031-5.
- Majeed, T., J. C. McConnell, and R. V. Yelle (1991). “Vibrationally excited H<sub>2</sub> in the outer planets thermosphere: Fluorescence in the Lyman and Werner bands”. In: *Planetary and Space Science* 39.11, pp. 1591–1606. doi: 10.1016/0032-0633(91)90085-o.
- Mandt, K. E. et al. (2012). “Ion densities and composition of Titan’s upper atmosphere derived from the Cassini Ion Neutral Mass Spectrometer: Analysis methods and comparison of measured ion densities to photochemical model simulations”. In: *Journal of Geophysical Research: Planets* 117.E10. doi: 10.1029/2012je004139.
- Matcheva, K. I. and D. J. Barrow (2012). “Small-scale variability in Saturn’s lower ionosphere”. In: *Icarus* 221.2, pp. 525–543. doi: 10.1016/j.icarus.2012.08.022.
- McElroy, D. et al. (2013). “The UMIST database for astrochemistry 2012”. In: *Astronomy and Astrophysics* 550, A36, A36. doi: 10.1051/0004-6361/201220465.
- McElroy, M. B. (1973). “The ionospheres of the major planets”. In: *Space Science Reviews* 14.3, pp. 460–473. doi: 10.1007/bf00214756.

- Millar, T. J., C. Walsh, and T. A. Field (2017). “Negative Ions in Space”. In: *Chemical Reviews* 117.3, pp. 1765–1795. doi: 10.1021/acs.chemrev.6b00480.
- Miller, K. et al. (2020). “Cassini INMS constraints on the composition and latitudinal fractionation of Saturn ring rain material”. In: *Icarus* 339, p. 113595. doi: 10.1016/j.icarus.2019.113595.
- Mitchell, D. G. et al. (2018). “Dust grains fall from Saturn’s D-ring into its equatorial upper atmosphere”. In: *Science* 362.6410. doi: 10.1126/science.aat2236.
- Moore, L. et al. (2018). “Models of Saturn’s Equatorial Ionosphere Based on In Situ Data From Cassini’s Grand Finale”. In: *Geophysical Research Letters* 45.18, pp. 9398–9407. doi: 10.1029/2018gl078162.
- Moore, L. et al. (2004). “Modeling of global variations and ring shadowing in Saturn’s ionosphere”. In: *Icarus* 172.2, pp. 503–520. doi: 10.1016/j.icarus.2004.07.007.
- Moore, L. et al. (2006). “Cassini radio occultations of Saturn’s ionosphere: Model comparisons using a constant water flux”. In: *Geophysical Research Letters* 33.22. doi: 10.1029/2006gl027375.
- Moore, L. et al. (2010). “Latitudinal variations in Saturn’s ionosphere: Cassini measurements and model comparisons”. In: *Journal of Geophysical Research: Space Physics* 115.11, pp. 1–12. doi: 10.1029/2010ja015692.
- Morooka, M. W. et al. (2019). “Saturn’s Dusty Ionosphere”. In: *Journal of Geophysical Research: Space Physics* 124.3, pp. 1679–1697. doi: 10.1029/2018ja026154.
- Moses, J. I. and S. F. Bass (2000). “The effects of external material on the chemistry and structure of Saturn’s ionosphere”. In: *Journal of Geophysical Research: Planets* 105.E3, pp. 7013–7052. doi: 10.1029/1999je001172.
- Moses, J. I. et al. (2023). “Saturn’s atmospheric response to the large influx of ring material inferred from Cassini INMS measurements”. In: *Icarus* 391, p. 115328. doi: 10.1016/j.icarus.2022.115328.
- Mott-Smith, H. M. and I. Langmuir (1926). “The Theory of Collectors in Gaseous Discharges”. In: *Phys. Rev.* 28 (4), pp. 727–763. doi: 10.1103/PhysRev.28.727.
- Müller-Wodarg, I. C. F. et al. (2006). “A global circulation model of Saturn’s thermosphere”. In: *Icarus* 180.1, pp. 147–160. doi: 10.1016/j.icarus.2005.09.002.
- Müller-Wodarg, I. C. F. et al. (2012). “Magnetosphere–atmosphere coupling at Saturn: 1 – Response of thermosphere and ionosphere to steady state polar forcing”. In: *Icarus* 221.2, pp. 481–494. doi: 10.1016/j.icarus.2012.08.034.
- Müller-Wodarg, I. C. F. et al. (2019). “Atmospheric Waves and Their Possible Effect on the Thermal Structure of Saturn’s Thermosphere”. In: *Geophysical Research Letters* 46.5. doi: 10.1029/2018gl081124.

- Nagy, A. F. et al. (2006). “First results from the ionospheric radio occultations of Saturn by the Cassini spacecraft”. In: *Journal of Geophysical Research: Space Physics* 111.A6. doi: 10.1029/2005ja011519.
- Northrop, T. and J. Connerney (1987). “A micrometeorite erosion model and the age of Saturn’s rings”. In: *Icarus* 70.1, pp. 124–137. doi: 10.1016/0019-1035(87)90079-0.
- O’Donoghue, J. et al. (2013). “The domination of Saturn’s low-latitude ionosphere by ring ‘rain’”. In: *Nature* 496.7444, pp. 193–195. doi: 10.1038/nature12049.
- O’Donoghue, J. et al. (2017). “Redetection of the Ionospheric H<sub>3</sub><sup>+</sup> Signature of Saturn’s “Ring Rain””. In: *Geophysical Research Letters* 44.23. doi: 10.1002/2017g1075932.
- O’Donoghue, J. et al. (2019). “Observations of the chemical and thermal response of ‘ring rain’ on Saturn’s ionosphere”. In: *Icarus* 322. doi: 10.1016/j.icarus.2018.10.027.
- Perry, M. E. et al. (2018). “Material Flux From the Rings of Saturn Into Its Atmosphere”. In: *Geophysical Research Letters* 45.19. doi: 10.1029/2018g1078575.
- Persoon, A. M. et al. (2005). “Equatorial electron density measurements in Saturn’s inner magnetosphere”. In: *Geophysical Research Letters* 32.23. doi: 10.1029/2005g1024294.
- Persoon, A. M. et al. (2013). “The plasma density distribution in the inner region of Saturn’s magnetosphere”. In: *Journal of Geophysical Research: Space Physics* 118.6, pp. 2970–2974. doi: 10.1002/jgra.50182.
- Persoon, A. M. et al. (2019). “Electron Density Distributions in Saturn’s Ionosphere”. In: *Geophysical Research Letters* 46.6. doi: 10.1029/2018g1078020.
- Poppe, A. R. (2016). “An improved model for interplanetary dust fluxes in the outer Solar System”. In: *Icarus* 264, pp. 369–386. doi: 10.1016/j.icarus.2015.10.001.
- Prasad, S. S. and W. T. Huntress (1980). “A model for gas phase chemistry in interstellar clouds: I. The basic model, library of chemical reactions, and chemistry among C, N, and O compounds.” In: *The Astrophysical Journal Supplement Series* 43, pp. 1–35. doi: 10.1086/190665.
- Rees, M. H. (1989). *Physics and Chemistry of the Upper Atmosphere*. Cambridge Atmospheric and Space Science Series. Cambridge University Press. doi: 10.1017/cbo9780511573118.
- Roussos, E. et al. (2018). “A radiation belt of energetic protons located between Saturn and its rings”. In: *Science* 362.6410. doi: 10.1126/science.aat1962.
- Schunk, R. and A. Nagy (2009). *Ionospheres: Physics, Plasma Physics, and Chemistry*. 2nd ed. Cambridge Atmospheric and Space Science Series. Cambridge University Press. doi: 10.1017/cbo9780511635342.
- Serigano, J. et al. (2022). “Compositional Measurements of Saturn’s Upper Atmosphere and Rings From Cassini INMS: An Extended Analysis of Mea-

- surements From Cassini’s Grand Finale Orbits”. In: *Journal of Geophysical Research: Planets* 127.6, e2022JE007238. doi: 10.1029/2022je007238.
- Shebanits, O. (2017). “Titan’s ionosphere and dust : – as seen by a space weather station”. PhD thesis. Uppsala University, Swedish Institute of Space Physics, Uppsala Division.
- Sheppard, S. S. et al. (2023). “New Jupiter and Saturn Satellites Reveal New Moon Dynamical Families”. In: *Research Notes of the AAS* 7.5, p. 100. doi: 10.3847/2515-5172/acd766.
- Spilker, L. (2019). “Cassini-Huygens’ exploration of the Saturn system: 13 years of discovery”. In: *Science* 364.6445, pp. 1046–1051. doi: 10.1126/science.aat3760.
- Srama, R. et al. (2004). “The Cassini Cosmic Dust Analyzer”. In: *Space Science Reviews* 114.1, pp. 465–518. doi: 10.1007/s11214-004-1435-z.
- Sulaiman, A. H. et al. (2017). “Intense Harmonic Emissions Observed in Saturn’s Ionosphere”. In: *Geophysical Research Letters* 44.24. doi: 10.1002/2017gl1076184.
- Teodoro, L. F. A. et al. (2023). “A Recent Impact Origin of Saturn’s Rings and Mid-sized Moons”. In: *The Astrophysical Journal* 955.2, p. 137. doi: 10.3847/1538-4357/acf4ed.
- Thomas, L. and M. R. Bowman (1985). “Model studies of the D-region negative-ion composition during day-time and night-time”. In: *Journal of Atmospheric and Terrestrial Physics* 47.6, pp. 547–556. doi: 10.1016/0021-9169(85)90037-6.
- Tiscareno, M. S. et al. (2019). “Close-range remote sensing of Saturn’s rings during Cassini’s ring-grazing orbits and Grand Finale”. In: *Science* 364.6445, eaau1017. doi: 10.1126/science.aau1017.
- Tokar, R. L. et al. (2005). “Cassini observations of the thermal plasma in the vicinity of Saturn’s main rings and the F and G rings”. In: *Geophysical Research Letters* 32.14. doi: 10.1029/2005gl1022690.
- Verbiscer, A. J., M. F. Skrutskie, and D. P. Hamilton (2009). “Saturn’s largest ring”. In: *Nature* 461.7267, pp. 1098–1100. doi: 10.1038/nature08515.
- Vigren, E. et al. (2022). “Empirical Photochemical Modeling of Saturn’s Ionization Balance Including Grain Charging”. In: *The Planetary Science Journal* 3.2, p. 49. doi: 10.3847/psj/ac4eee.
- Wahlund, J. et al. (2009). “Detection of dusty plasma near the E-ring of Saturn”. In: *Planetary and Space Science* 57.14-15, pp. 1795–1806. doi: 10.1016/j.pss.2009.03.011.
- Wahlund, J. et al. (2018). “In situ measurements of Saturn’s ionosphere show that it is dynamic and interacts with the rings”. In: *Science* 359.6371, pp. 66–68. doi: 10.1126/science.aao4134.
- Waite, J. H., S. K. Atreya, and A. F. Nagy (1979). “The ionosphere of Saturn: Predictions for Pioneer 11”. In: *Geophysical Research Letters* 6.9, pp. 723–726. doi: 10.1029/GL006i009p00723.

- Waite, J. H. et al. (2004). “The Cassini Ion and Neutral Mass Spectrometer (INMS) Investigation”. In: *Space Science Reviews* 114.1-4, pp. 113–231. doi: 10.1007/s11214-004-1408-2.
- Waite, J. H. et al. (2018). “Chemical interactions between Saturn’s atmosphere and its rings”. In: *Science* 362.6410. doi: 10.1126/science.aat2382.
- Wakelam, V. et al. (2012). “A Kinetic Database For Astrochemistry (Kida)”. In: *The Astrophysical Journal Supplement Series* 199.1, p. 21. doi: 10.1088/0067-0049/199/1/21.
- Whiter, D. K. et al. (2021). “Fine-scale dynamics of fragmented aurora-like emissions”. In: *Annales Geophysicae* 39.6, pp. 975–989. doi: 10.5194/angeo-39-975-2021.
- Wisdom, J. et al. (2022). “Loss of a satellite could explain Saturn’s obliquity and young rings”. In: *Science* 377.6612, pp. 1285–1289. doi: 10.1126/science.abn1234.
- Woods, T. N. et al. (2005). “Solar EUV Experiment (SEE): Mission overview and first results”. In: *Journal of Geophysical Research: Space Physics* 110.A1. doi: 10.1029/2004ja010765.
- Yelle, R. V. et al. (2018). “Thermal Structure and Composition of Saturn’s Upper Atmosphere From Cassini/Ion Neutral Mass Spectrometer Measurements”. In: *Geophysical Research Letters* 45.20. doi: 10.1029/2018gl1078454.
- Young, D. T. et al. (2004). “Cassini Plasma Spectrometer Investigation”. In: *Space Science Reviews* 114.1, pp. 1–112. doi: 10.1007/s11214-004-1406-4.
- Zhang, Z. et al. (2017a). “Cassini microwave observations provide clues to the origin of Saturn’s C ring”. In: *Icarus* 281, pp. 297–321. doi: 10.1016/j.icarus.2016.07.020.
- Zhang, Z. et al. (2017b). “Exposure age of Saturn’s A and B rings, and the Cassini Division as suggested by their non-icy material content”. In: *Icarus* 294, pp. 14–42. doi: 10.1016/j.icarus.2017.04.008.
- Zhang, Z. et al. (2021). “Particle-in-cell simulations of the Cassini spacecraft’s interaction with Saturn’s ionosphere during the Grand Finale”. In: *Monthly Notices of the Royal Astronomical Society* 504.1, pp. 964–973. doi: 10.1093/mnras/stab750.
- Zhang, Z. et al. (2023). “Simulating Secondary Electron and Ion Emission from the Cassini Spacecraft in Saturn’s Ionosphere”. In: *The Planetary Science Journal* 4.6, p. 105. doi: 10.3847/PSJ/acd844.

# Acta Universitatis Upsaliensis

*Digital Comprehensive Summaries of Uppsala Dissertations from the Faculty of Science and Technology 2313*

Editor: The Dean of the Faculty of Science and Technology

A doctoral dissertation from the Faculty of Science and Technology, Uppsala University, is usually a summary of a number of papers. A few copies of the complete dissertation are kept at major Swedish research libraries, while the summary alone is distributed internationally through the series Digital Comprehensive Summaries of Uppsala Dissertations from the Faculty of Science and Technology. (Prior to January, 2005, the series was published under the title “Comprehensive Summaries of Uppsala Dissertations from the Faculty of Science and Technology”.)

Distribution: [publications.uu.se](http://publications.uu.se)  
urn:nbn:se:uu:diva-512834



ACTA UNIVERSITATIS  
UPSALIENSIS  
2023